

Precision calculations of $B \rightarrow K^*$ form factors from SCET sum rules beyond leading-power contributions

Jing Gao[Ⓛ],^a Ulf-G. Meißner[Ⓛ],^{a,b,c} Yue-Long Shen[Ⓛ]^d and Dong-Hao Li[Ⓛ],^{e,*}

^a Helmholtz-Institut für Strahlen- und Kernphysik and Bethe Center for Theoretical Physics, Universität Bonn, D-53115 Bonn, Germany

^b Institute for Advanced Simulation, Forschungszentrum Jülich, D-52425 Jülich, Germany

^c Peng Huanwu Collaborative Center for Research and Education, Beihang University, Beijing 100191, China

^d College of Physics and Photoelectric Engineering, Ocean University of China, Qingdao 266100, China

^e MOE Frontiers Science Center for Rare Isotopes, and School of Nuclear Science and Technology, Lanzhou University, Lanzhou 730000, China

E-mail: gao@hiskp.uni-bonn.de, meissner@hiskp.uni-bonn.de, shenylmeteor@ouc.edu.cn, lidh@lzu.edu.cn

ABSTRACT: We employ vacuum-to- B meson correlation functions with interpolating currents $\bar{q}'\not{q}$ and $\bar{q}'\not{\gamma}_\perp q$ to construct light-cone sum rules (LCSR) for calculating the $B \rightarrow K^*$ form factors in the large recoil region. We investigate several subleading-power corrections to these form factors at tree level, including the next-to-leading power contributions from the hard-collinear propagator, the subleading power corrections from the effective current $\bar{q}\Gamma[i\not{D}_\perp/(2m_b)]h_v$, and four-body higher-twist effects. By utilizing the available leading-power results at $\mathcal{O}(\alpha_s)$ and the power corrections from higher-twist B -meson light-cone distribution amplitudes from our previous work, we further derive the improved numerical predictions for $B \rightarrow K^*$ form factors by applying the three-parameter model for B -meson light-cone distribution amplitudes (LCDAs). The subleading-power contribution is about 30% relative to the corresponding leading-power result. Taking the well-adopted Bourrely-Caprini-Lellouch (BCL) parametrization, we then provide the numerical results of $B \rightarrow K^*$ form factors in the entire kinematic range, by adopting the combined fit to both LCSR predictions and lattice QCD results. Taking advantage of the newly obtained $B \rightarrow K^*$ form factors, we analyse the rare exclusive decay $B \rightarrow K^*\nu_\ell\bar{\nu}_\ell$ and estimate the Standard Model predictions of $\mathcal{BR}(\bar{B}^0 \rightarrow \bar{K}^{*0}\nu_\ell\bar{\nu}_\ell) = 7.54(86) \times 10^{-6}$, $\mathcal{BR}(\bar{B}^+ \rightarrow \bar{K}^{*+}\nu_\ell\bar{\nu}_\ell) = 9.35(94) \times 10^{-6}$ and longitudinal K^* polarization fraction $F_L = 0.44(4)$.

*Corresponding author

Contents

1	Introduction	2
2	NLL correction to the $B \rightarrow K^*$ form factors at leading power	3
3	Subleading-power contributions	6
3.1	Higher-twist B -meson LCDA contribution	7
3.2	Higher-order terms in hard-collinear propagator	9
3.3	Subleading heavy-quark effective current	11
3.4	Higher-twist four-particle contribution	12
4	Numerical analysis	14
4.1	Theory inputs	14
4.2	Numerical predictions for the $B \rightarrow K^*$ form factors	17
4.3	Phenomenological analysis of the $B \rightarrow K^* \nu_\ell \bar{\nu}_\ell$ observables	22
5	Conclusions	24
A	Hard function for the SCET currents at $\mathcal{O}(\alpha_s)$	30
B	Effective B-meson distribution amplitudes	30
C	Dispersion integral formula	31
D	Modeling the B-meson LCDAs	31

1 Introduction

The semi-leptonic B decays induced by the flavor-changing neutral current (FCNC), combined with clean experimental signals, are among the most powerful probes of physics beyond the Standard Model (SM). In the flagship semi-leptonic $b \rightarrow s\ell^+\ell^-$ decays, several flavor anomalies have been observed, including a $\mathcal{O}(4\sigma)$ deviation of the experimental measured $\mathcal{BR}(B^+ \rightarrow K^+\mu^+\mu^-)$ compared to Standard Model predictions in the low q^2 region, where q denotes the momentum of the lepton pair, and the inconsistency between the angular observable $P'_5(B \rightarrow K^{*0}\mu^+\mu^-)$ measured by the LHCb collaboration and the SM computations in two q^2 bins [1–3]. Notably, the branching ratio of $B \rightarrow K\nu_\ell\bar{\nu}_\ell$ reported by the Belle II collaboration exceeds the Standard Model prediction by 2.7σ [1, 4]. B -meson decays with a pair of neutrinos in the final state are one of the cleanest channels in the Standard Model, since the electroweak effects in these processes are under control and the QCD effects are fully encoded in the corresponding hadronic form factors. Meanwhile, the $b \rightarrow s\ell^+\ell^-$ decays are affected by various “non-factorizable” contributions, including the short-distance hard spectator scattering and weak annihilation effects, and the power suppressed long-distance quark loop contribution [5, 6]. Studying the $b \rightarrow s\nu\bar{\nu}$ process allows us to distinguish among different Z' models that were introduced to explain the anomalies in $b \rightarrow s\ell^+\ell^-$, or further constrain the Wilson coefficients of high-dimensional operators within the Standard Model effective field theory [6–8].

In order to make precise theoretical predictions for observables in $B \rightarrow K^*\nu_\ell\bar{\nu}_\ell$ decay, precision calculations of $B \rightarrow K^*$ form factors play an essential role. In the high q^2 region, the form factors have been computed using lattice QCD simulations in Refs. [9, 10], and these results need to be extrapolated to cover the entire kinetic region, which introduces some model-dependence. In the low q^2 region, QCD based methods have been developed to address the factorization formulas involved in the heavy-to-light transition processes with the help of the heavy quark expansion. At leading power in Λ_{QCD}/m_Q , the heavy-to-light form factors can be expressed as a product of the effective operators in soft-collinear effective theory (SCET), the so-called A0-type and B1-type SCET operators, and corresponding coefficient functions with hard fluctuations [11–14],

$$F_i^{B \rightarrow V}(n \cdot p) = C_i^{(\text{A0})}(n \cdot p)\xi_a(n \cdot p) + \int d\tau C_i^{(\text{B1})}(\tau, n \cdot p)\Xi_a(\tau, n \cdot p), \quad (a = \parallel, \perp), \quad (1.1)$$

where $C_i^{(\text{A0})}$ and $C_i^{(\text{B1})}$ are the hard functions corresponding to A0-type and B1-type operators and their specific expressions up to $\mathcal{O}(\alpha_s)$ can be found in Appendix A [15–18]. Suffering from the endpoint divergences appearing in the convolution of the jet functions and the light-cone distribution amplitudes, the soft-collinear factorization of form factors ξ_a cannot be achieved directly. On the contrary, the B1-type effective matrix elements can be expressed as the convolution of jet functions and hadronic distribution amplitudes.

Starting from the vacuum-to-light-meson correlation functions with heavy meson interpolating current, LCSR with light-meson distribution amplitudes results for $B \rightarrow V$ form factors up to twist-4 at tree level and to twist-2 at $\mathcal{O}(\alpha_s)$ have been studied in Refs. [5, 19–21]. Following the analogous strategies, the QCD/SCET light-cone sum rules for B -meson decay form factors can be derived at leading-logarithmic accuracy in Refs. [22, 23] and next-to-leading-logarithmic accuracy in Ref. [24]. These computations depend on the universal B -meson distribution amplitudes with duality assumption of the light-meson channel and the narrow-width approximation for the vector mesons [25, 26]. The finite-width effects in the $B \rightarrow K^*$ form factors were investigated in Refs. [27, 28]. Beyond the leading power, the power corrections to $B \rightarrow V$ form factors from two-particle and three-particle higher-twist B -meson LCDAs have been computed in Ref. [24]. Compared to QCD factorization, the endpoint singularity is eliminated in the LCSR approach, albeit at the cost of introducing a systematic uncertainty stemming from the assumption of quark-

hadron duality above a continuum threshold s_0 in order to determine the lowest-lying hadronic parameters.

This work aims to systematically investigate the subleading power effects of $B \rightarrow K^*$ form factors in QCD by constructing sum rules with B -meson DAs, following the program pursued in Refs. [29–31]. The subleading power corrections considered in the present work arise from three distinct sources: (I) the power-suppressed terms from the heavy quark expansion of the hard-collinear propagator, (II) the subleading effective current $\bar{q}\Gamma[i\cancel{D}_\perp/(2m_b)]h_v$ from the weak current $\bar{q}\Gamma b$, (III) the twist-five and twist-six four-particle distribution amplitudes. By employing combined fits with lattice QCD results in the high q^2 region and the improved LCSR form factors in the low q^2 region with the BCL parametrization [32–36], we provide the central values and correlation matrix of the BCL z -expansion coefficients. We then explore the observables in the $\bar{B} \rightarrow \bar{K}^*\nu_\ell\bar{\nu}_\ell$ process, including the differential branching ratios and the longitudinal K^* polarization fraction.

The organization of the article is outlined as follows: In the section 2, we present the definitions, notations and leading power effective SCET form factors at $\mathcal{O}(\alpha_s)$. Section 3 shows the computation of various power-suppressed contributions and present the corresponding $B \rightarrow K^*$ form factors with LCSR. In section 4, we perform the BCL parametrization and obtain the z -series expansion coefficients and their correlation matrix by a combined fit of form factors from lattice QCD and LCSR. The updated predictions for the branching ratio $\bar{B} \rightarrow \bar{K}^*\nu_\ell\bar{\nu}_\ell$ and longitudinal K^* polarization fraction are also included. Finally in Section 5, we discuss our results and future prospects. Various technical details are collected in the Appendix.

2 NLL correction to the $B \rightarrow K^*$ form factors at leading power

According to the standard Lorentz decomposition of the bilinear quark currents, the $B \rightarrow K^*$ form factors are defined in the standard way [11]

$$\begin{aligned}
c_V \langle V(p, \varepsilon^*) | \bar{q}\gamma_\mu b | \bar{B}(p+q) \rangle &= -\frac{2iV(q^2)}{m_B + m_V} \epsilon_{\mu\nu\rho\sigma} \varepsilon^{*\nu} p^\rho q^\sigma, \\
c_V \langle V(p, \varepsilon^*) | \bar{q}\gamma_\mu \gamma_5 b | \bar{B}(p+q) \rangle &= \frac{2m_V \varepsilon^* \cdot q}{q^2} q_\mu A_0(q^2) \\
&\quad + (m_B + m_V) \left(\varepsilon_\mu^* - \frac{\varepsilon^* \cdot q}{q^2} q_\mu \right) A_1(q^2) \\
&\quad - \frac{\varepsilon^* \cdot q}{m_B + m_V} \left[(2p+q)_\mu - \frac{m_B^2 - m_V^2}{q^2} q_\mu \right] A_2(q^2), \\
c_V \langle V(p, \varepsilon^*) | \bar{q}i\sigma_{\mu\nu} q^\nu b | \bar{B}(p+q) \rangle &= 2iT_1(q^2) \epsilon_{\mu\nu\rho\sigma} \varepsilon^{*\nu} p^\rho q^\sigma, \\
c_V \langle V(p, \varepsilon^*) | \bar{q}i\sigma_{\mu\nu} \gamma_5 q^\nu b | \bar{B}(p+q) \rangle &= T_2(q^2) [(m_B^2 - m_V^2) \varepsilon_\mu^* - (\varepsilon^* \cdot q)(2p+q)_\mu] \\
&\quad + T_3(q^2) (\varepsilon^* \cdot q) \left[q_\mu - \frac{q^2}{m_B^2 - m_V^2} (2p+q)_\mu \right],
\end{aligned} \tag{2.1}$$

with the convention $\epsilon_{0123} = -1$. The factor c_V denotes the flavor structure of a vector meson with $c_V = 1$ for the K^* meson. Further, m_V and m_B denote the mass of K^* meson and B -meson respectively. p and q are corresponding to the momentum of K^* meson and momentum transfer of weak current as well as $q = p_B - p = m_{B^*} - p$. In the following subsection, the calligraphic form factors \mathcal{F}_i represent the linear combinations of the conventionally defined form factors in Eq. (2.1),

$$\begin{aligned}
\mathcal{V}(q^2) &= \frac{m_B}{m_B + m_V} V(q^2), & \mathcal{A}_0(q^2) &= \frac{m_V}{E_V} A_0(q^2), & \mathcal{A}_1(q^2) &= \frac{m_B + m_V}{2E_V} A_1(q^2), \\
\mathcal{A}_2(q^2) &= \frac{m_B - m_V}{m_B} A_2(q^2), & \mathcal{T}_1(q^2) &= T_1(q^2), & \mathcal{T}_2(q^2) &= \frac{m_B}{2E_V} T_2(q^2), \\
\mathcal{A}_{12}(q^2) &= \mathcal{A}_1(q^2) - \mathcal{A}_2(q^2), & \mathcal{T}_{23}(q^2) &= \mathcal{T}_2(q^2) - \mathcal{T}_3(q^2).
\end{aligned} \tag{2.2}$$

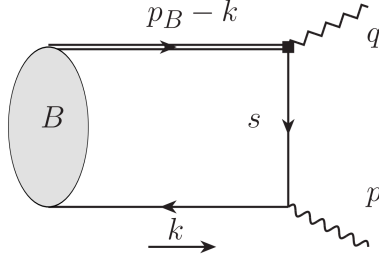


Figure 1. Diagrammatic representations of the vacuum-to- B meson correlation functions at tree level, where double line stands for the effective heavy quark field in HQET, the wave line indicates the interpolating current and square box denotes the weak vertex.

Following the procedure outlined in Refs. [37–40], we can construct the vacuum-to- B -meson correlation functions as

$$\begin{aligned}\Pi_{\nu\mu,\parallel}(p, q) &= \int d^4x e^{ip \cdot x} \langle 0 | T \{ j_\nu(x), \bar{q}(0) \Gamma_\mu^{(a)} b(0) \} | \bar{B} \rangle, \\ \Pi_{\nu\delta\mu,\perp}(p, q) &= \int d^4x e^{ip \cdot x} \langle 0 | T \{ j_{\nu\delta}(x), \bar{q}(0) \Gamma_\mu^{(a)} b(0) \} | \bar{B} \rangle,\end{aligned}\tag{2.3}$$

where $j_\nu(x) = \bar{q}'(x) \gamma_\nu q(x)$ and $j_{\nu\delta}(x) = \bar{q}'(x) \gamma_\nu \gamma_\delta q(x)$ are the interpolating currents corresponding to the longitudinal and transverse polarization vector meson state with momentum p , respectively. We further introduce two light-cone vectors n_μ and \bar{n}_μ which satisfy the relations $n \cdot \bar{n} = 2$, $n \cdot n = \bar{n} \cdot \bar{n} = 0$. The power corrections arising from the interpolating currents were not considered in section 3, thus we keep the leading-power term in the extrapolation current for simplicity. Then the correlation functions in Eq. (2.3) can be expressed as

$$\Pi_{\nu\mu,\parallel}^{(a)}(p, q) = \bar{n}_\nu \Pi_{\mu,\parallel}^{(a)}(p, q), \quad \Pi_{\delta\mu,\perp}^{(a)}(p, q) = \bar{n}_\nu \Pi_{\delta\mu,\perp}^{(a)}(p, q),\tag{2.4}$$

with

$$\begin{aligned}\Pi_{\mu,\parallel}^{(a)}(p, q) &= \int d^4x e^{ip \cdot x} \langle 0 | T \{ \bar{q}'(x) \frac{\not{n}}{2} q(x), \bar{q}(0) \Gamma_\mu^{(a)} b(0) \} | \bar{B}(p+q) \rangle, \\ \Pi_{\delta\mu,\perp}^{(a)}(p, q) &= \int d^4x e^{ip \cdot x} \langle 0 | T \{ \bar{q}'(x) \frac{\not{n}}{2} \gamma_\delta q(x), \bar{q}(0) \Gamma_\mu^{(a)} b(0) \} | \bar{B}(p+q) \rangle.\end{aligned}\tag{2.5}$$

For convenience, we consider the decay process in the rest frame of B -meson, allowing us to get the four-velocity vector of B -meson as $v_\mu = p_B/m_B = (n_\mu + \bar{n}_\mu)/2$. In this process, we adopt the following power counting scheme for the momentum of interpolating current and masses of hard-collinear strange quark propagator and spectator quark of B -meson

$$n \cdot p \sim \mathcal{O}(m_b), \quad |\bar{n} \cdot p| \sim \mathcal{O}(\Lambda_{\text{QCD}}/m_b), \quad m_q \sim m_{q'} \sim \mathcal{O}(\Lambda_{\text{QCD}}/m_b).\tag{2.6}$$

Performing the two-step matching process $\text{QCD} \rightarrow \text{SCET}_I \rightarrow \text{SCET}_{II}$, the correlation functions defined in Eq. (2.3) can be presented with SCET_I operators, the SCET Lagrangian [41] and effective currents [14]. After employing the operator product expansion (OPE) to the correlation functions in the region of $p^2 < 0$ and inserting the two-particle leading-twist B -meson LCDA [11, 42]

$$\langle 0 | (\bar{q}_s Y_s)_\beta (t \bar{n}) (Y_s^\dagger h_v)_\alpha (0) | \bar{B}_v \rangle = -\frac{i \tilde{f}_B(\mu) m_B}{4} \left\{ \frac{1 + \not{v}}{2} [2 \tilde{\phi}_B^+(t, \mu) + (\tilde{\phi}_B^-(t, \mu) - \tilde{\phi}_B^+(t, \mu)) \not{v}] \gamma_5 \right\}_{\alpha\beta},\tag{2.7}$$

where

$$\tilde{\phi}_B^\pm(t) \equiv \int_0^\infty d\omega e^{-i\omega t} \phi_B^\pm(\omega), \quad (2.8)$$

we can evaluate the leading-power contribution of the correlation function in Eq. (2.3) up to $\mathcal{O}(\alpha_s)$ [24]. The tree level Feynmann diagram is shown in Fig. 1. The scale-dependent decay constant $\tilde{f}_B(\mu)$ in HQET has the following relation with the decay constant f_B in QCD

$$\tilde{f}_B(\mu) = f_B \left[1 - \frac{\alpha_s C_F}{4\pi} \left(3 \ln \frac{m_b}{\mu} - 2 \right) + \mathcal{O}(\alpha_s^2) \right]. \quad (2.9)$$

At the hadronic level, the correlation function with different interpolating currents can be expressed by the following formulas

$$\begin{aligned} \Pi_{\mu,\parallel}^{(V-A)}(p, q) &= \frac{f_V^\parallel m_V}{m_V^2/n \cdot p - \bar{n} \cdot p - i0} \left(\frac{n \cdot p}{2m_V} \right)^2 \left\{ \frac{m_B}{m_B - n \cdot p} n_\mu \left[\left(-\frac{2m_V}{n \cdot p} A_0(q^2) \right) \right. \right. \\ &\quad \left. \left. + \left(\frac{m_B + m_V}{n \cdot p} A_1(q^2) - \frac{m_B - m_V}{m_B} A_2(q^2) \right) \right] \right. \\ &\quad \left. - \bar{n}_\mu \left[\left(\frac{2m_V}{n \cdot p} A_0(q^2) \right) + \left(\frac{m_B + m_V}{n \cdot p} A_1(q^2) - \frac{m_B - m_V}{m_B} A_2(q^2) \right) \right] \right\} \\ &\quad + \int d\omega' \frac{1}{\omega' - \bar{n} \cdot p - i0} \left[n_\mu \varrho_{n,\parallel}^{(V-A)}(\omega', n \cdot p) + \bar{n}_\mu \varrho_{\bar{n},\parallel}^{(V-A)}(\omega', n \cdot p) \right], \\ \Pi_{\delta\mu,\perp}^{(V-A)}(p, q) &= -\frac{1}{2} \frac{f_V^\perp n \cdot p}{m_V^2/n \cdot p - \bar{n} \cdot p - i0} \\ &\quad \times \left[g_{\delta\mu}^\perp \left(\frac{m_B + m_V}{n \cdot p} A_1(q^2) \right) + i\epsilon_{\delta\mu}^\perp \left(\frac{m_B}{m_B + m_V} V(q^2) \right) \right] \\ &\quad + \int d\omega' \frac{1}{\omega' - \bar{n} \cdot p - i0} \left[g_{\delta\mu}^\perp \varrho_{\perp,A_1}^{(V-A)}(\omega', n \cdot p) + i\epsilon_{\delta\mu}^\perp \varrho_{\perp,V}^{(V-A)}(\omega', n \cdot p) \right], \\ \Pi_{\mu,\parallel}^{(T+\bar{T})}(p, q) &= \frac{1}{2} \frac{f_V^\parallel m_V}{m_V^2/n \cdot p - \bar{n} \cdot p - i0} \left(\frac{n \cdot p}{2m_V} \right)^2 \\ &\quad \times [n \cdot q \bar{n}_\mu - \bar{n} \cdot q n_\mu] \left[\frac{m_B}{n \cdot p} T_2(q^2) - T_3(q^2) \right] \\ &\quad + \int d\omega' \frac{1}{\omega' - \bar{n} \cdot p - i0} [n \cdot q \bar{n}_\mu - \bar{n} \cdot q n_\mu] \varrho_{\parallel}^{(T+\bar{T})}(\omega', n \cdot p), \\ \Pi_{\delta\mu,\perp}^{(T+\bar{T})}(p, q) &= \frac{1}{2} \frac{f_V^\perp n \cdot p m_B}{m_V^2/n \cdot p - \bar{n} \cdot p - i0} \left[g_{\delta\mu}^\perp \left(\frac{m_B}{n \cdot p} T_2(q^2) \right) + i\epsilon_{\delta\mu}^\perp T_1(q^2) \right] \\ &\quad + \int d\omega' \frac{1}{\omega' - \bar{n} \cdot p - i0} \left[g_{\delta\mu}^\perp \varrho_{\perp,T_2}^{(T+\bar{T})}(\omega', n \cdot p) + i\epsilon_{\delta\mu}^\perp \varrho_{\perp,T_1}^{(T+\bar{T})}(\omega', n \cdot p) \right], \end{aligned} \quad (2.10)$$

where the definitions of decay constant for the longitudinal and transverse K^* meson are [43]

$$\begin{aligned} \langle 0 | \bar{q}'(x) \frac{\not{h}}{2} q(x) | V(p, \varepsilon) \rangle &= \frac{i}{2} f_V^\parallel m_V n \cdot \varepsilon, \\ \langle 0 | \bar{q}'(x) \frac{\not{h}}{2} \gamma_\delta^\perp q(x) | V(p, \varepsilon) \rangle &= -n \cdot p \frac{i}{2} f_V^\perp \varepsilon_\delta^\perp(p). \end{aligned} \quad (2.11)$$

To extract the form factors of the $B \rightarrow K^*$ process, we utilize a dispersion relation and express the partonic correlation function in the form of a dispersion integral

$$\Pi(n \cdot p, \bar{n} \cdot p) = \frac{1}{\pi} \int_0^\infty d\omega' \frac{\text{Im} \Pi(n \cdot p, \omega')}{\omega' - \bar{n} \cdot p - i\epsilon}, \quad (2.12)$$

then apply quark-hadron duality and Borel transformation to both the partonic correlation function and hadronic correlation function of the SCET representation in order to eliminate the continuum and resonance contributions and reduce the uncertainties from the duality ansatz. We finally obtain the four effective SCET form factors at $\mathcal{O}(\alpha_s)$ [24]

$$\begin{aligned} \xi_{\parallel, \text{NLL}}(n \cdot p) &= \frac{U_2(\mu_{h2}, \mu) \tilde{f}_B(\mu_{h2}) 2m_B m_V}{f_V^{\parallel}} \frac{1}{(n \cdot p)^2} \\ &\times \int_0^{\omega_s^{\parallel}} d\omega' \exp\left[-\frac{n \cdot p\omega' - m_V^2}{n \cdot p\omega_M}\right] [\phi_{B, \text{eff}}^-(\omega', \mu) + \phi_{B, m}^+(\omega', \mu)], \end{aligned} \quad (2.13)$$

$$\begin{aligned} \xi_{\perp, \text{NLL}}(n \cdot p) &= \frac{U_2(\mu_{h2}, \mu) \tilde{f}_B(\mu_{h2}) m_B}{f_V^{\perp}(\nu)} \frac{1}{n \cdot p} \\ &\times \int_0^{\omega_s^{\perp}} d\omega' \exp\left[-\frac{n \cdot p\omega' - m_V^2}{n \cdot p\omega_M}\right] \tilde{\phi}_{B, \text{eff}}^-(\omega', \mu, \nu), \end{aligned} \quad (2.14)$$

$$\begin{aligned} \Xi_{\parallel, \text{NLL}}(n \cdot p) &= -\frac{\alpha_s C_F}{\pi} \frac{U_2(\mu_{h2}, \mu) \tilde{f}_B(\mu_{h2}) m_B m_V}{f_V^{\parallel}} \frac{1}{n \cdot p m_b} [(1 - \tau)\theta(\tau)\theta(1 - \tau)] \\ &\times \int_0^{\omega_s^{\parallel}} d\omega' \exp\left[-\frac{n \cdot p\omega' - m_V^2}{n \cdot p\omega_M}\right] \int_{\omega'}^{\infty} d\omega \frac{\phi_B^+(\omega, \mu)}{\omega}, \end{aligned} \quad (2.15)$$

$$\begin{aligned} \Xi_{\perp, \text{NLL}}(n \cdot p) &= -\frac{\alpha_s C_F}{2\pi} \frac{U_2(\mu_{h2}, \mu) \tilde{f}_B(\mu_{h2}) m_B}{f_V^{\perp}(\nu)} \frac{1}{m_b} [(1 - \tau)\theta(\tau)\theta(1 - \tau)] \\ &\times \int_0^{\omega_s^{\perp}} d\omega' \exp\left[-\frac{n \cdot p\omega' - m_V^2}{n \cdot p\omega_M}\right] \int_{\omega'}^{\infty} d\omega \frac{\phi_B^+(\omega, \mu)}{\omega}, \end{aligned} \quad (2.16)$$

where $\omega_s^{\parallel, \perp} = s_0^{\parallel, \perp}/n \cdot p$ and $\omega_M = M^2/n \cdot p$ denote the effective threshold and Borel mass, respectively, which are two fundamental inputs of LCSR. μ and ν correspond to the factorization scale and renormalization scale, in order. Besides, the effective B -meson distribution amplitudes are introduced to describe both the hard-collinear and soft fluctuations [24, 39], which are given in Appendix B.

Because the hard functions $C_i^{(A0)}$ and $C_i^{(B1)}$ contain the enhanced logarithms term $\ln^n(m_b/\Lambda_{\text{QCD}})$, we solve the RG evolution equations to sum them up to all orders in perturbation theory at NLL and LL accuracy [16]. The general solutions to the RG equations are

$$C_i^{(A0)}(n \cdot p, \mu) = U_1(n \cdot p, \mu_h, \mu) C_i^{(A0)}(n \cdot p, \mu_h), \quad (2.17)$$

$$C_i^{(B1)}(n \cdot p, \tau, \mu) = \exp[-S(n \cdot p, \mu_h, \mu)] \int_0^1 d\tau' U_i^{(B1)}(\tau, \tau', \mu_h, \mu) C_i^{(B1)}(n \cdot p, \tau', \mu_h), \quad (2.18)$$

where the NLL resummation evolution factor U_1 and LL expansion of the S function can be found in Refs. [16, 44]. Adopting the effective SCET form factors and resummation improved hard functions, we can derive the $B \rightarrow K^*$ form factors in QCD at NLL accuracy with the relations that have been computed in Ref. [24].

3 Subleading-power contributions

In this section, we investigate the power correction arising from various sources to the $B \rightarrow K^*$ form factors within the LCSR approach. Taking advantage of the classical equation of motion in HQET and the factorization formula of correlation functions at subleading power, we ultimately obtain the tree-level power correction to the $B \rightarrow K^*$ form factors in the large hadronic recoil region and analyze the corresponding scaling behavior.

3.1 Higher-twist B -meson LCDA contribution

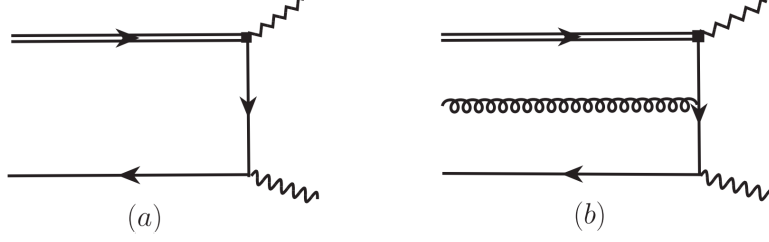


Figure 2. Diagrammatic representations of two-particle (left) and three-particle (right) corrections to the vacuum-to-bottom meson correlation functions at tree level, where the square box indicates the weak vertex and waveline stands for the interpolating current.

The sources of higher-twist B -meson LCDA contributions arise from two-particle and three-particle higher-twist B -meson LCDAs as illustrated in Fig. 2. The definition of the light-cone expansion of the quark propagator in the background gluon field can be found in Ref. [45]

$$\langle 0|T\{\bar{q}(x), q(0)\}|0\rangle \supset ig_s \int \frac{d^4l}{(2\pi)^4} e^{-il \cdot x} \int_0^1 du \left[\frac{ux_\mu \gamma_\nu}{l^2 - m_q^2} - \frac{(l + m_q)\sigma_{\mu\nu}}{2(l^2 - m_q^2)^2} \right] G^{\mu\nu}(ux), \quad (3.1)$$

and the general parameterization of the vacuum-to- B -meson matrix element of three-body HQET operator is given by Ref. [46]

$$\begin{aligned} \langle 0|\bar{q}_\alpha(z_1\bar{n})g_s G^{\mu\nu}(z_2\bar{n})h_{v\beta}|0\rangle &= \frac{\tilde{f}_B(\mu)m_B}{4} [(1 + \not{v})\{(v_\mu\gamma_\nu - v_\nu\gamma_\mu) [\Psi_A(z_1, z_2, \mu) - \Psi_V(z_1, z_2, \mu)] \\ &- i\sigma_{\mu\nu}\Psi_V(z_1, z_2, \mu) - (\bar{n}_\mu v_\nu - \bar{n}_\nu v_\mu)X_A(z_1, z_2, \mu) + (\bar{n}_\mu\gamma_\nu - \bar{n}_\nu\gamma_\mu) [W(z_1, z_2, \mu) + Y_A(z_1, z_2, \mu)] \\ &+ i\epsilon_{\mu\nu\alpha\beta}\bar{n}^\alpha v^\beta \gamma_5 \tilde{X}_A(z_1, z_2, \mu) - i\epsilon_{\mu\nu\alpha\beta}\bar{n}^\alpha \gamma^\beta \gamma_5 \tilde{Y}_A(z_1, z_2, \mu) \\ &- (\bar{n}_\mu v_\nu - \bar{n}_\nu v_\mu)\not{n}W(z_1, z_2, \mu) + (\bar{n}_\mu\gamma_\nu - \bar{n}_\nu\gamma_\mu)\not{n}Z(z_1, z_2, \mu)\}\gamma_5]_{\beta\alpha}, \end{aligned} \quad (3.2)$$

where $\epsilon_{0123} = -1$, and we also introduce three-particle HQET distribution amplitudes with the definite collinear twist in our work

$$\begin{aligned} \Phi_3 &= \Psi_A - \Psi_V, & \Phi_4 &= \Psi_A + \Psi_V, \\ \Psi_4 &= \Psi_A + X_A, & \tilde{\Psi}_4 &= \Psi_V - \tilde{X}_A, \\ \tilde{\Phi}_5 &= \Psi_A + \Psi_V + 2Y_A - 2\tilde{Y}_A + 2W, & \Psi_5 &= -\Psi_A + X_A - 2Y_A, \\ \tilde{\Psi}_5 &= -\Psi_V - \tilde{X}_A + 2\tilde{Y}_A, & \Phi_6 &= \Psi_A - \Psi_V + 2Y_A + 2W + 2\tilde{Y}_A - 4Z. \end{aligned} \quad (3.3)$$

First, we evaluate the correlation function $\Pi_{\parallel}(p, q)$ in Eq. (2.5), which corresponds to the longitudinally polarized vector meson. After inserting the propagator in Eq. (3.1) and applying the three-particle higher-twist B -meson LCDA in Eq. (3.2), the three-particle higher-twist correction to the correlation functions can be written as

$$\Pi_{\parallel, \text{NLP}}^{(a), 3\text{PHT}}(p, q) = \frac{\tilde{f}_B(\mu)m_B}{2n \cdot p} \left[\Gamma_{\parallel}^{(a)} \Pi_{\parallel, \text{NLP}}^{3\text{PHT}} + \tilde{\Gamma}_{\parallel}^{(a)} \tilde{\Pi}_{\parallel, \text{NLP}}^{3\text{PHT}} \right], \quad (3.4)$$

with

$$\begin{aligned} \Pi_{\parallel, \text{NLP}}^{3\text{PHT}} &= \int_0^\infty d\omega_1 \int_0^\infty d\omega_2 \int_0^1 du \frac{-2\bar{u}\Phi_4(\omega_1, \omega_2)}{(\bar{n} \cdot p - \omega_1 - u\omega_2 - \omega_q)^2} + \frac{m_q}{n \cdot p} \frac{\Psi_5(\omega_1, \omega_2) - \tilde{\Psi}_5(\omega_1, \omega_2)}{(\bar{n} \cdot p - \omega_1 - u\omega_2 - \omega_q)^2}, \\ \tilde{\Pi}_{\parallel, \text{NLP}}^{3\text{PHT}} &= \int_0^\infty d\omega_1 \int_0^\infty d\omega_2 \int_0^1 du \frac{\tilde{\Psi}_5(\omega_1, \omega_2) - (2u - 1)\Phi_5(\omega_1, \omega_2)}{(\bar{n} \cdot p - \omega_1 - u\omega_2 - \omega_q)^2} - \frac{m_q}{n \cdot p} \frac{2\tilde{\Phi}_6(\omega_1, \omega_2)}{(\bar{n} \cdot p - \omega_1 - u\omega_2 - \omega_q)^2}, \end{aligned} \quad (3.5)$$

and the factors $\Gamma_{\parallel}^{(a)}$, $\tilde{\Gamma}_{\parallel}^{(a)}$ take the form

$$\left\{ \Gamma_{\parallel}^{(V-A)}, \Gamma_{\parallel}^{(T+\tilde{T})} \right\} \in \left\{ n_{\mu}, \bar{n}_{\mu} \frac{n \cdot q}{2} - n_{\mu} \frac{\bar{n} \cdot q}{2} \right\}, \quad \left\{ \tilde{\Gamma}_{\parallel}^{(V-A)}, \tilde{\Gamma}_{\parallel}^{(T+\tilde{T})} \right\} \in \left\{ \bar{n}_{\mu}, n_{\mu} \frac{\bar{n} \cdot q}{2} - \bar{n}_{\mu} \frac{n \cdot q}{2} \right\}, \quad (3.6)$$

where $a \in \{V-A, T + \tilde{T}\}$ denotes the different Dirac structures $\gamma_{\mu}(1 - \gamma_5)$ and $i\sigma_{\mu\nu}(1 + \gamma_5)q^{\nu}$ of the heavy-to-light weak current, respectively. Besides, we set $\omega_q = m_q^2/n \cdot p$ for brevity.

Along the same lines, the three-particle higher-twist correction to the correlation function $\Pi_{\perp}(p, q)$ in Eq. (2.5), which corresponds to a transversely polarized vector meson, can be expressed as

$$\Pi_{\perp, \text{NLP}}^{(a), 3\text{PHT}}(p, q) = \frac{\tilde{f}_B(\mu)m_B}{2n \cdot p} \int_0^{\infty} d\omega_1 \int_0^{\infty} d\omega_2 \int_0^1 du \left[\Gamma_{\perp}^{(a)} \frac{(1 - 2u)\Psi_5(\omega_1, \omega_2) - \tilde{\Psi}_5(\omega_1, \omega_2)}{(\bar{n} \cdot p - \omega_1 - u\omega_2 - \omega_q)^2} \right. \\ \left. - \tilde{\Gamma}_{\perp}^{(a)} \frac{m_q}{n \cdot p} \frac{\Psi_5(\omega_1, \omega_2) + \tilde{\Psi}_5(\omega_1, \omega_2)}{(\bar{n} \cdot p - \omega_1 - u\omega_2 - \omega_q)^2} \right] \quad (3.7)$$

by taking $\epsilon_{\delta\mu}^{\perp} \equiv \frac{1}{2}\epsilon_{\delta\mu\rho\sigma}n^{\rho}\bar{n}^{\sigma}$ and

$$\left\{ \Gamma_{\perp}^{(V-A)}, \Gamma_{\perp}^{(T+\tilde{T})} \right\} \in \{g_{\delta\mu}^{\perp} + i\epsilon_{\delta\mu}, g_{\delta\mu}^{\perp} - i\epsilon_{\delta\mu}^{\perp}\}, \\ \left\{ \tilde{\Gamma}_{\perp}^{(V-A)}, \tilde{\Gamma}_{\perp}^{(T+\tilde{T})} \right\} \in \{-\bar{n} \cdot q(g_{\delta\mu}^{\perp} + i\epsilon_{\delta\mu}), n \cdot q(g_{\delta\mu}^{\perp} - i\epsilon_{\delta\mu}^{\perp})\}. \quad (3.8)$$

In addition, the two-particle higher-twist B -meson LCDA, for example $g_B^{\pm}(\omega)$, also generates subleading-power contributions. The off-light-cone corrections to the renormalized two-body non-local HQET matrix element at $\mathcal{O}(x^2)$ accuracy is given by Ref. [46]

$$\langle 0 | (\bar{q}_s Y_s)_{\beta}(x) (Y_s^{\dagger} h_v)_{\alpha} | \bar{B}_v \rangle = -i \frac{\tilde{f}_B(\mu)m_B}{4} \int_0^{\infty} d\omega e^{-i\omega v \cdot x} \left[\frac{1 + \not{x}}{2} \left\{ 2 \left[\phi_B^+(\omega, \mu) + x^2 g_B^+(\omega, \mu) \right] \right. \right. \\ \left. \left. - \frac{\not{x}}{v \cdot x} \left[(\phi_B^+(\omega, \mu) - \phi_B^-(\omega, \mu)) + x^2 (g_B^+(\omega, \mu) - g_B^-(\omega, \mu)) \right] \right\} \gamma_5 \right]_{\alpha\beta}, \quad (3.9)$$

where the higher-twist LCDA $g_B^-(\omega, \mu)$ can be decomposed into the ‘‘genuine’’ twist-five three-particle LCDAs $\Psi_5(\omega_1, \omega_2, \mu)$ and the lower-twist ‘‘Wandzura-Wilczek’’ two-particle LCDAs $\hat{g}_B^-(\omega, \mu)$ [46]

$$g_B^-(x) = \hat{g}_B^-(x) - \frac{1}{2} \int_0^1 du \bar{u} \Psi_5(x, ux). \quad (3.10)$$

After inserting the two-particle higher-twist B -meson LCDA in Eq. (3.9) to the correlation functions, we therefore obtain the factorization formulas for the two-particle higher-twist contribution

$$\Pi_j^{(a), 2\text{PHT}}(p, q) = \frac{\tilde{f}_B(\mu)m_B}{2n \cdot p} \Gamma_j^{(a)} \left\{ \int_0^{\infty} d\omega \frac{4\hat{g}_B^-(\omega, \mu)}{(\bar{n} \cdot p - \omega)^2} \right. \\ \left. - \int_0^{\infty} d\omega_1 \int_0^{\infty} d\omega_2 \int_0^1 du \frac{2\bar{u}\Psi_5(\omega_1, \omega_2)}{(\bar{n} \cdot p - \omega_1 - u\omega_2)^2} \right\}, \quad (3.11)$$

with $\Gamma_{\parallel}^{(a)} \in \{\bar{n}_{\mu}, n_{\mu} \frac{\bar{n} \cdot q}{2} - \bar{n}_{\mu} \frac{n \cdot q}{2}\}$ and $\Gamma_{\perp}^{(a)} \in \{g_{\delta\mu}^{\perp} + i\epsilon_{\delta\mu}^{\perp}, -\bar{n} \cdot q(g_{\delta\mu}^{\perp} + i\epsilon_{\delta\mu}^{\perp})\}$ for $a \in \{V-A, T + \tilde{T}\}$ and $j = \parallel, \perp$.

Combining the two-particle and three-particle higher-twist contributions, we obtain the higher-twist corrections to the correlation functions $\Pi_{\parallel, \perp}^{(a)}(p, q)$ at tree level. We then implement the

dispersion relation to the correlation functions at the partonic level and apply the quark-hadron duality ansatz and Borel transformation. This process results in the following sum rules for the higher-twist contributions to the $B \rightarrow K^*$ form factors [24]

$$\begin{aligned}
& f_V^\perp \exp \left[-\frac{m_V^2}{n \cdot p \omega_M} \right] \{ \mathcal{V}_{\text{NLP}}^{\text{HT}}(q^2), \mathcal{A}_{1,\text{NLP}}^{\text{HT}}(q^2), \mathcal{T}_{1,\text{NLP}}^{\text{HT}}(q^2), \mathcal{T}_{2,\text{NLP}}^{\text{HT}}(q^2) \} \\
&= \frac{\tilde{f}_B(\mu) m_B}{(n \cdot p)^2} \left\{ f_{2,1}[\tau_1] + f_{3,2}[\tau_2] - \kappa_i \frac{m_q}{n \cdot p} f_{3,2}[\tau_2] \right\}, \\
& f_V^\parallel \exp \left[-\frac{m_V^2}{n \cdot p \omega_M} \right] \{ \mathcal{A}_{0,\text{NLP}}^{\text{HT}}(q^2), \mathcal{A}_{12,\text{NLP}}^{\text{HT}}(q^2), \mathcal{T}_{23,\text{NLP}}^{\text{HT}}(q^2) \} \\
&= \frac{2\tilde{f}_B(\mu) m_B m_V}{(n \cdot p)^3} \left\{ f_{2,1}[\tau_1] + f_{3,2}[\tau_3] + \frac{m_q}{n \cdot p} f_{3,2}[\tau_4] + \iota_i \left(f_{3,2}[\tau_4] + \frac{m_q}{n \cdot p} f_{3,2}[-\tau_3] \right) \right\},
\end{aligned} \tag{3.12}$$

with the symmetry-breaking factors

$$\kappa_i \in \left\{ +1, -1, \frac{n \cdot q}{\bar{n} \cdot q}, -\frac{n \cdot q}{\bar{n} \cdot q} \right\}, \quad \iota_i \in \left\{ \frac{n \cdot q}{m_B}, -\frac{n \cdot q}{m_B}, 1 \right\}, \tag{3.13}$$

and the function $f_{i,j}$ denotes the contribution of i -particle LCDA term with the power j in the denominators $\phi(\omega)/(\omega - \dots)^j$, whose explicit expressions are listed in Appendix C. Further, the explicit density functions are expressed by

$$\begin{aligned}
\tau_1(\omega) &= -4 \frac{d}{d\omega} \hat{g}_B^-(\omega), \quad \tau_2(\omega_1, \omega_2, u) = 2\bar{u}\Phi_4(\omega_1, \omega_2), \quad \tau_3(\omega_1, \omega_2, u) = 2\Phi_6(\omega_1, \omega_2), \\
\tau_4(\omega_1, \omega_2, u) &= \Psi_5(\omega_1, \omega_2) + \tilde{\Psi}_5(\omega_1, \omega_2) - \frac{4\bar{u}\omega_q}{\bar{n} \cdot p - \omega_1 - u\omega_2 - \omega_q} \Psi_5(\omega_1, \omega_2).
\end{aligned} \tag{3.14}$$

3.2 Higher-order terms in hard-collinear propagator

Following the strategy outlined in Refs. [47, 48], we proceed with the calculation of the sub-leading power corrections arising from the hard-collinear propagator expansion in the correlation functions

$$\begin{aligned}
\Pi_{\mu,\parallel}^{(a)}(p, q) &= \int d^4x e^{ip \cdot x} \langle 0 | T \{ \bar{q}'(x) \frac{\not{q}}{2} q(x), \bar{q}(0) \Gamma_\mu^{(a)} b(0) \} | \bar{B}(p+q) \rangle, \\
\Pi_{\delta\mu,\perp}^{(a)}(p, q) &= \int d^4x e^{ip \cdot x} \langle 0 | T \{ \bar{q}'(x) \frac{\not{q}}{2} \gamma_{\delta\perp} q(x), \bar{q}(0) \Gamma_\mu^{(a)} b(0) \} | \bar{B}(p+q) \rangle,
\end{aligned} \tag{3.15}$$

where the Dirac structures of heavy-to-light weak current are

$$\Gamma_\mu^{(a)} \in \{ \gamma_\mu(1 - \gamma_5), i\sigma_{\mu\nu}(1 + \gamma_5)q^\nu \}. \tag{3.16}$$

Expanding the hard-collinear propagator in the correlation functions given by Eq. (3.15) in powers of Λ_{QCD}/m_b , we obtain

$$\frac{\not{p} - \not{k} + m_q}{(p-k)^2 - m_q^2 + i\epsilon} = \frac{\overbrace{\left[n \cdot p \frac{\not{q}}{2} + (\bar{n} \cdot p \frac{\not{q}}{2} - \not{k} + m_q) \right]}^{\text{LP}} + \overbrace{\left[\frac{n \cdot p \frac{\not{q}}{2} \bar{n} \cdot p n \cdot k}{n \cdot p(\bar{n} \cdot p - \bar{n} \cdot k)} + \frac{n \cdot p \frac{\not{q}}{2} (m_q^2 - m_{q'}^2)}{n \cdot p(\bar{n} \cdot p - \bar{n} \cdot k)} \right]}^{\text{NLP}}}{n \cdot p(\bar{n} \cdot p - \bar{n} \cdot k)}, \tag{3.17}$$

where m_q is the mass of hard-collinear strange quark propagator and $m_{q'}$ is the mass of spectator quark of the B -meson. “LP” refers to the leading-power effect of hard-collinear propagator in the tree level contribution, while “NLP” represents the subleading power contribution resulting from the expansion of the hard-collinear propagator.

We then insert the subleading-power terms into the correlation functions $\Pi_{\parallel,\perp}^{(a)}$, and apply the HQET operator identities [46, 49]

$$\begin{aligned}
v_\rho \frac{\partial}{\partial x_\rho} \bar{q}(x) \Gamma[x, 0] h_v(0) &= v \cdot \partial \bar{q}(x) \Gamma[x, 0] h_v(0) + i \int_0^1 du \bar{u} \bar{q}(x)[x, ux] x^\lambda g_s G_{\lambda\rho}(ux) [ux, 0] v^\rho \Gamma h_v(0), \\
iv \cdot \partial \langle 0 | \bar{q}(x) \Gamma[x, 0] h_v(0) | \bar{B}_v \rangle &= \bar{\Lambda} \langle 0 | \bar{q}(x) \Gamma[x, 0] h_v(0) | \bar{B}_v \rangle, \\
\frac{\partial}{\partial x_\rho} \bar{q}(x) \gamma_\rho \Gamma[x, 0] h_v(0) &= -i \int_0^1 du u \bar{q}(x)[x, ux] x^\lambda g_s G_{\lambda\rho}(ux) [ux, 0] \gamma^\rho \Gamma h_v(0) + im_{q'} \bar{q}(x) \Gamma[x, 0] h_v(0).
\end{aligned} \tag{3.18}$$

Taking advantage of the three-body light-cone HQET matrix element up to twist-six accuracy in Eq. (3.2), we can derive the expressions for the first NLP term presented in Eq. (3.17),

$$\begin{aligned}
\Pi_{\text{NLP}}^{\text{I,QPE}} &= \left[\frac{\tilde{f}_B(\mu) m_B}{2n \cdot p} \right] \left\{ \int_0^\infty d\omega \frac{(\omega - 2\bar{\Lambda}) \phi_B^+(\omega)}{\bar{n} \cdot p - \omega} + (m_{q'} - m_q) \int_0^\infty d\omega \frac{\phi_B^-(\omega)}{\bar{n} \cdot p - \omega} \right. \\
&\quad \left. - \int_0^1 du \int_0^\infty d\omega_1 \int_0^\infty d\omega_2 \frac{2[u\Phi_4(\omega_1, \omega_2) + \Psi_4(\omega_1, \omega_2)]}{(\bar{n} \cdot p - \omega_1 - u\omega_2)^2} \right\}, \\
\tilde{\Pi}_{\text{NLP}}^{\text{I,QPE}} &= \left[\frac{\tilde{f}_B(\mu) m_B}{2n \cdot p} \right] \left\{ \int_0^\infty d\omega \frac{(\omega - 2\bar{\Lambda})}{\bar{n} \cdot p - \omega} \phi_B^-(\omega) \right. \\
&\quad \left. - \int_0^1 du \int_0^\infty d\omega_1 \int_0^\infty d\omega_2 \frac{2\bar{u}\Psi_5(\omega_1, \omega_2)}{(\bar{n} \cdot p - \omega_1 - u\omega_2)^2} \right\},
\end{aligned} \tag{3.19}$$

with the hadronic parameter $\bar{\Lambda}$ characterizing the ‘‘effective mass’’ of the B -meson state in HQET. It can be defined as [50]

$$\bar{\Lambda} \equiv \frac{\langle 0 | \bar{q} i v \cdot \overleftarrow{D} \Gamma h_v | \bar{B}_q(v) \rangle}{\langle 0 | \bar{q} i \Gamma h_v | \bar{B}_q(v) \rangle}. \tag{3.20}$$

Noticing the relation $n_\alpha = 2v_\alpha - \bar{n}_\alpha$, we can further compute the second NLP term contribution along the same lines,

$$\begin{aligned}
\Pi_{\text{NLP}}^{\text{II,QPE}} = 0, \quad \tilde{\Pi}_{\text{NLP}}^{\text{II,QPE}} &= \left[\frac{\tilde{f}_B(\mu) m_B}{2n \cdot p} \right] \left\{ \int_0^\infty d\omega \frac{\bar{n} \cdot p (2\bar{\Lambda} - \omega)}{(\bar{n} \cdot p - \omega)^2} \phi_B^-(\omega) \right. \\
&\quad \left. + \int_0^1 du \int_0^\infty d\omega_1 \int_0^\infty d\omega_2 \frac{4\bar{u} \bar{n} \cdot p \Psi_5(\omega_1, \omega_2)}{(\bar{n} \cdot p - \omega_1 - u\omega_2)^3} \right\}.
\end{aligned} \tag{3.21}$$

Then the third contribution of the NLP term in the hard-collinear propagator expansion can be easily derived by applying the standard factorization procedure,

$$\Pi_{\text{NLP}}^{\text{III,QPE}} = 0, \quad \tilde{\Pi}_{\text{NLP}}^{\text{III,QPE}} = (m_q^2 - m_{q'}^2) \int_0^\infty d\omega \frac{1}{(\bar{n} \cdot p - \omega)^2} \phi_B^-(\omega). \tag{3.22}$$

We can finally get the factorization formulae of the NLP contributions resulting from the quark propagator expansion at tree level

$$\Pi_{j,\text{NLP}}^{(a),\text{QPE}} = \Gamma_j^{(a)} (\Pi_{\text{NLP}}^{\text{I,QPE}} + \Pi_{\text{NLP}}^{\text{II,QPE}} + \Pi_{\text{NLP}}^{\text{III,QPE}}) + \tilde{\Gamma}_j^{(a)} (\tilde{\Pi}_{\text{NLP}}^{\text{I,QPE}} + \tilde{\Pi}_{\text{NLP}}^{\text{II,QPE}} + \tilde{\Pi}_{\text{NLP}}^{\text{III,QPE}}), \tag{3.23}$$

by taking

$$\Gamma_{\parallel,\perp}^{(\text{V-A})} = \{n_\mu, g_{\delta\mu}^\perp - i\epsilon_{\delta\mu}^\perp\}, \quad \tilde{\Gamma}_{\parallel,\perp}^{(\text{V-A})} = \{\bar{n}_\mu, g_{\delta\mu}^\perp + i\epsilon_{\delta\mu}^\perp\} \tag{3.24}$$

and

$$\begin{aligned}
\Gamma_{\parallel,\perp}^{(\text{T}+\hat{\text{T}})} &= - \left\{ n_\mu \frac{\bar{n} \cdot q}{2} - \bar{n}_\mu \frac{n \cdot q}{2}, (g_{\delta\mu}^\perp - i\epsilon_{\delta\mu}^\perp) \frac{n \cdot q}{2} \right\}, \\
\tilde{\Gamma}_{\parallel,\perp}^{(\text{T}+\hat{\text{T}})} &= - \left\{ \bar{n}_\mu \frac{n \cdot q}{2} - n_\mu \frac{\bar{n} \cdot q}{2}, (g_{\delta\mu}^\perp + i\epsilon_{\delta\mu}^\perp) \frac{\bar{n} \cdot q}{2} \right\}.
\end{aligned} \tag{3.25}$$

Adopting the standard LCSR strategy, we establish the correlation functions in the dispersion form and match it to the hadronic representation from in Eq. (2.10). Finally, we obtain the desired $B \rightarrow K^*$ form factors for the power-suppressed contribution arising from expanded hard-collinear propagator

$$f_V \exp \left[-\frac{m_V^2}{n \cdot p \omega_M} \right] \mathcal{F}_{i,\text{NLP}}^{\text{QPE}}(q^2) = \frac{\tilde{f}_B(\mu)m_B}{(n \cdot p)^2} \{ \kappa_i (f_{2,1}[\boldsymbol{\eta}_1] - f_{3,2}[\boldsymbol{\eta}_2]) + \tilde{\kappa}_i (f_{2,1}[\boldsymbol{\eta}_3] + f_{3,2}[\boldsymbol{\eta}_4] - f_{2,2}[\boldsymbol{\eta}_5] - f_{3,3}[\boldsymbol{\eta}_6]) \}, \quad (3.26)$$

where form factors $\mathcal{F}_i \in \{\mathcal{V}, \mathcal{A}_1, \mathcal{T}_1, \mathcal{T}_2, \mathcal{A}_0, \mathcal{A}_{12}, \mathcal{T}_{23}\}$ with the replacement $f_V \rightarrow f_V^\perp$ for the first four \mathcal{F}_i and $f_V \rightarrow f_V^\parallel$ for the last three \mathcal{F}_i , and the corresponding symmetry-breaking factors read

$$\kappa_i \in \left\{ -1, -1, -\frac{n \cdot q}{2m_B}, \frac{n \cdot q}{2m_B}, -\frac{m_V n \cdot q}{m_B n \cdot p}, -\frac{m_V n \cdot q}{m_B n \cdot p}, \frac{2m_V}{n \cdot p} \right\}, \quad (3.27)$$

$$\tilde{\kappa}_i \in \left\{ 1, -1, \frac{\bar{n} \cdot q}{2m_B}, \frac{\bar{n} \cdot q}{2m_B}, -\frac{m_V}{n \cdot p}, -\frac{m_V}{n \cdot p}, -\frac{2m_V}{n \cdot p} \right\}, \quad (3.28)$$

and the density function $\boldsymbol{\eta}_i$ are given as follows

$$\begin{aligned} \boldsymbol{\eta}_1(\omega) &= (\omega - 2\bar{\Lambda})\phi_B^+(\omega) + (m_{q'} - m_q)\phi_B^-(\omega), & \boldsymbol{\eta}_2(\omega_1, \omega_2, u) &= 2[u\Phi_4(\omega_1, \omega_2) + \Psi_4(\omega_1, \omega_2)], \\ \boldsymbol{\eta}_3(\omega) &= 0, & \boldsymbol{\eta}_4(\omega_1, \omega_2, u) &= 2\bar{u}\Psi_5(\omega_1, \omega_2), \\ \boldsymbol{\eta}_5(\omega) &= \omega(2\bar{\Lambda} - \omega)\phi_B^-(\omega) - (m_q^2 - m_{q'}^2)\phi_B^-(\omega), & \boldsymbol{\eta}_6(\omega_1, \omega_2, u) &= 2(\omega_1 + u\omega_2)\boldsymbol{\eta}_4(\omega_1, \omega_2, u). \end{aligned} \quad (3.29)$$

3.3 Subleading heavy-quark effective current

Now we proceed to take into account the subleading term of heavy-to-light effective current, which generates the power-suppressed contribution to the $B \rightarrow K^*$ form factors. In HQET, the bottom quark can be replaced by effective heavy quark field, and the heavy-to-light weak current is expanded to NLP [49]:

$$\bar{q}\Gamma_\mu b = \underbrace{\bar{q}\Gamma_\mu h_v}_{\text{LP}} + \underbrace{\frac{1}{2m_b}\bar{q}\Gamma_\mu i\overleftrightarrow{D}h_v}_{\text{NLP}} + \dots, \quad (3.30)$$

where $\overleftrightarrow{D} = \overrightarrow{D} - (v \cdot D)\not{v}$ and $\overleftrightarrow{D}h_v(0) = [\overrightarrow{D} - (v \cdot D)\not{v}]h_v(0) = \overrightarrow{D}h_v(0)$ due to the HQET EOM. The ellipses denote the terms in powers of $\mathcal{O}(1/m_b^2)$, whose contributions to the correlation functions are beyond the accuracy of our current work. Substituting the heavy-to-light effective current in the correlation function with the NLP term and taking advantage of the operator identities in Eq. (3.18) and Eq. (3.31),

$$\begin{aligned} \bar{q}(x)\Gamma[x, 0]\overrightarrow{D}_\rho h_v(0) &= \partial_\rho[\bar{q}(x)\Gamma[x, 0]h_v(0)] + i \int_0^1 du \bar{u}\bar{q}(x)[x, ux]g_s G_{\lambda\rho}(ux)[ux, 0]x^\lambda \Gamma h_v(0) \\ &\quad - \frac{\partial}{\partial x^\rho} \bar{q}(x)\Gamma[x, 0]h_v(0). \end{aligned} \quad (3.31)$$

It is straightforward to express the correlation functions in the following form

$$\begin{aligned} \Pi_{j,\text{NLP}}^{(a),\text{HQE}}(p, q) &= \int d^4x e^{ip \cdot x} \langle 0 | T \{ \bar{q}'(x)\Gamma_j q(x), \frac{1}{2m_b} \bar{q}(0)\Gamma_\mu^{(a)} i\overleftrightarrow{D}h_v \} | \bar{B}(p+q) \rangle \\ &= \frac{-1}{2m_b} \int d^4x \int \frac{d^4k}{(2\pi)^4} \frac{e^{ik \cdot x}}{\bar{n} \cdot p - \bar{n} \cdot k + i\epsilon} \left\{ \partial_\xi [\bar{q}(x)\Gamma_j \frac{\not{q}}{2}\Gamma_\mu^{(a)} \gamma_\xi h_v(0)] \right. \\ &\quad \left. + i \int_0^1 du \bar{u}\bar{q}(x)x^\rho g_s G_{\rho\xi}(ux)\Gamma_j \frac{\not{q}}{2}\Gamma_\mu^{(a)} \gamma_\xi h_v(0) - \frac{\partial}{\partial x_\xi} [\bar{q}(x)]\Gamma_j \frac{\not{q}}{2}\Gamma_\mu^{(a)} \gamma_\xi h_v(0) \right\}, \end{aligned} \quad (3.32)$$

where $a \in \{V-A, T+\tilde{T}\}$ denotes the different Dirac structures $\Gamma_\mu^{(a)} \in \{\gamma_\mu(1-\gamma_5), i\sigma_{\mu\nu}(1+\gamma_5)q^\nu\}$ and $\Gamma_j \in \{\frac{\not{n}}{2}, \frac{\not{n}}{2}\gamma_\delta^\perp\}$ for $j = \parallel, \perp$, respectively. We can further derive the factorization formula utilizing analogous techniques at tree level,

$$\begin{aligned} \Pi_{j,\text{NLP}}^{(a),\text{HQE}} = & \Gamma_j^{(a)} \frac{\tilde{f}_B(\mu)m_B}{4m_b} \left\{ \int_0^\infty d\omega \frac{1}{\bar{n} \cdot p - \omega} [(2\bar{\Lambda} - \omega)\phi_B^+(\omega) + (\bar{\Lambda} - \omega - m_{q'})\phi_B^-(\omega)] \right. \\ & \left. + \int_0^\infty d\omega_1 \int_0^\infty d\omega_2 \int_0^1 du \frac{2[\Phi_4(\omega_1, \omega_2) + \Psi_4(\omega_1, \omega_2)]}{(\bar{n} \cdot p - \omega_1 - u\omega_2)^2} \right\}, \end{aligned} \quad (3.33)$$

by taking

$$\Gamma_j^{\text{V-A}} \in \{-\bar{n}_\mu, g_{\delta\mu}^\perp + i\epsilon_{\delta\mu}^\perp\}, \quad \Gamma_j^{\text{T}+\tilde{\text{T}}} \in \left\{ n_\mu \frac{\bar{n} \cdot q}{2} - \bar{n}_\mu \frac{n \cdot q}{2}, \bar{n} \cdot q (g_{\delta\mu}^\perp + i\epsilon_{\delta\mu}^\perp) \right\}. \quad (3.34)$$

Matching the partonic representation with the hadronic dispersion relations in Eq. (2.10) enables us to derive the subleading-power heavy-quark effective current correction to the $B \rightarrow K^*$ form factors

$$f_V \exp \left[-\frac{m_V^2}{n \cdot p \omega_M} \right] \mathcal{F}_{i,\text{NLP}}^{\text{HQE}}(q^2) = \frac{\tilde{f}_B(\mu)m_B}{2(n \cdot p)m_b} c_i \{f_{2,1}[\zeta_1] + f_{3,2}[\zeta_2]\}, \quad (3.35)$$

where the coefficient factors c_i are extracted from the correlation function at hadronic level,

$$c_i \in \left\{ -1, -1, \frac{\bar{n} \cdot q}{m_B}, \frac{\bar{n} \cdot q}{m_B}, \frac{m_V}{n \cdot p}, \frac{m_V}{n \cdot p}, \frac{2m_V}{n \cdot p} \right\}, \quad (3.36)$$

and the density functions ζ_i can be derived from the correlation function at the partonic level in Eq. (3.33),

$$\zeta_1(\omega) = (2\bar{\Lambda} - \omega)\phi_B^+(\omega) + (\bar{\Lambda} - \omega - m_{q'})\phi_B^-(\omega), \quad \zeta_2(\omega_1, \omega_2, u) = 2[\Phi_4(\omega_1, \omega_2) + \Psi_4(\omega_1, \omega_2)]. \quad (3.37)$$

Both the hard-collinear propagator correction and the subleading effective current correction to the $B \rightarrow K^*$ are in good agreement with the previous calculation for the $B \rightarrow D^*$ process as reported in Ref. [31], when the mass of charm quark is replaced by that of the strange quark.

3.4 Higher-twist four-particle contribution

We are now in the position to calculate the heavy-to-light B -meson decay form factors from the twist-five and twist-six four-particle LCDAs in the factorization approximation. These subleading power corrections of the form factors can be factorized as a product of the lower-twist two-particle LCDAs and the quark condensate [51]. By evaluating the lowest-order Feynmann diagrams shown in Fig. 3, one gets the non-leading Fock-state correction to the correlation function

$$\begin{aligned} \Pi_{j,\text{NLP}}^{(a),\text{AP}} = & \frac{g_s^2 C_F}{12} \frac{\tilde{f}_B(\mu)m_B}{n \cdot p} \left\{ \Gamma_j^{(a)} \langle \bar{q}q \rangle \int_0^\infty d\omega \frac{\phi_B^+(\omega)}{\bar{n} \cdot p(\omega - \bar{n} \cdot p)^2} \right. \\ & \left. + \tilde{\Gamma}_j^{(a)} \langle \bar{q}'q' \rangle \int_0^\infty d\omega \frac{\phi_B^+(\omega)}{\omega^3} \left[\frac{2\omega}{\bar{n} \cdot p - \omega} - \frac{\omega^2}{\bar{n} \cdot p(\bar{n} \cdot p - \omega)} + 2 \ln \frac{\bar{n} \cdot p - \omega}{\bar{n} \cdot p} \right] \right\}, \end{aligned} \quad (3.38)$$

with $\Gamma_\parallel^{(a)} = \tilde{\Gamma}_\parallel^{(a)} = \{\bar{n}_\mu, n_\mu \frac{\bar{n} \cdot q}{2} - \bar{n}_\mu \frac{n \cdot q}{2}\}$ and $\Gamma_\perp^{(a)} = 0$, $\tilde{\Gamma}_\perp^{(a)} = \{g_{\delta\mu}^\perp + i\epsilon_{\delta\mu}^\perp, -\bar{n} \cdot q (g_{\delta\mu}^\perp + i\epsilon_{\delta\mu}^\perp)\}$ for $a \in \{V-A, T+\tilde{T}\}$. Here, $\Gamma_j^{(a)}$ and $\tilde{\Gamma}_j^{(a)}$ denote the contribution from diagram-(d) and diagram-(f) in Fig. 3 respectively. Further, $\langle \bar{q}q \rangle$ and $\langle \bar{q}'q' \rangle$ are the quark condensate of the hard-collinear propagator and of the spectator quark of the B -meson.

It is perhaps worth mentioning that we treat diagram (e) in Fig. 3 with the familiar background-field expansion of the quark propagator on the light-cone [45]

$$\langle 0|T\{q(x), \bar{q}(0)\}|0\rangle \supset \frac{\Gamma(d/2-1)}{8\pi^{d/2}(-x^2)^{d/2-1}} \int_0^1 du \bar{u} \not{x} g_s D_\lambda G^{\lambda\rho}(ux) x_\rho + \frac{\Gamma(d/2-2)}{16\pi^{d/2}(-x^2)^{d/2-2}}$$

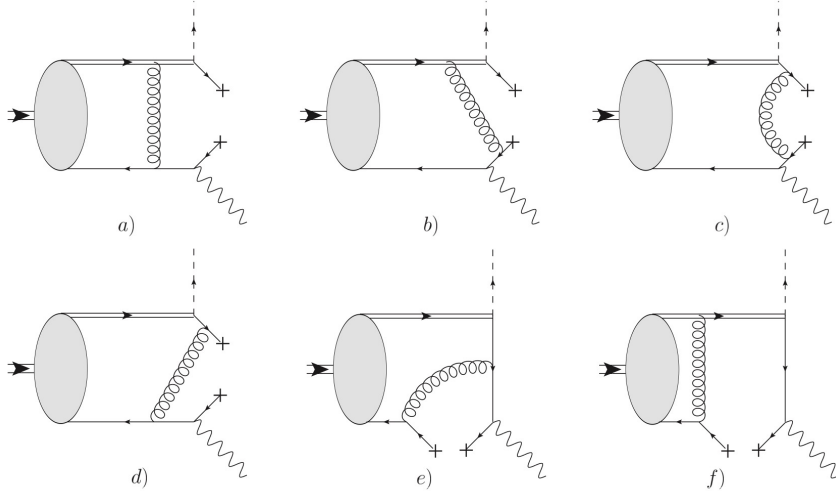


Figure 3. Diagrammatic representations of twist-five and twist-six four-particle corrections to the vacuum-to-bottom meson correlation functions.

$$\int_0^1 du (u\bar{u} - \frac{1}{2}) g_s D_\lambda G^{\lambda\rho}(ux) \gamma_\rho, \quad (3.39)$$

where the classical equation of motion in QCD is

$$D^\lambda G_{\lambda\rho}^a = -g_s \sum_q \bar{q} \gamma_\rho T^a q. \quad (3.40)$$

After explicitly calculating diagrams (a), (b) and (c) in Fig. 3, the results indicate that these three diagrams can only lead to the higher-power corrections compared to the main contributions from diagrams (d) and (e). The remaining diagram (f) turns out to be insensitive to both the hard and hard-collinear QCD dynamics. Besides, diagram (d) is power-suppressed compared to diagram (e) for the interpolating current corresponding to a transversely polarized vector meson.

With the dispersion transformation applied to the correlation functions at the partonic level and utilizing the standard sum rules strategy, we can derive the four-particle subleading-power corrections to the $B \rightarrow K^*$ form factors

$$f_V \exp \left[-\frac{m_V^2}{n \cdot p \omega_M} \right] \mathcal{F}_{i,\text{NLP}}^{4\text{P}}(q^2) = \frac{2\pi\alpha_s C_F \tilde{f}_B(\mu) m_B}{3(n \cdot p)^2} c_i \langle \bar{q} q' \rangle \left\{ \int_0^{\omega_s} d\omega \phi_{\text{eff-I}}^+(\omega) + \int_{\omega_s}^\infty d\omega \phi_{\text{eff-II}}^+(\omega) \right. \\ \left. - r_i \frac{\langle \bar{q} q \rangle}{\langle \bar{q}' q' \rangle} \left[e^{-\frac{\omega_s}{\omega_M}} \frac{\phi_B^+(\omega_s)}{\omega_s} - \int_{\omega_s}^\infty d\omega \frac{\phi_B^+(\omega)}{\omega^2} + \int_0^{\omega_s} d\omega \phi_{\text{eff-III}}^+(\omega) \right] \right\}, \quad (3.41)$$

where the coefficients

$$c_i \in \left\{ 1, 1, \frac{\bar{n} \cdot q}{m_B}, \frac{\bar{n} \cdot q}{m_B}, \frac{m_V}{n \cdot p}, \frac{m_V}{n \cdot p}, \frac{2m_V}{n \cdot p} \right\}, \quad r_i \in \{0, 0, 0, 0, 1, 1, 1\}, \quad (3.42)$$

for $\mathcal{F}_i \in \{\mathcal{V}, \mathcal{A}_1, \mathcal{T}_1, \mathcal{T}_2, \mathcal{A}_0, \mathcal{A}_{12}, \mathcal{T}_{23}\}$ and the explicit expressions for the density functions ϕ_{eff} are given by

$$\phi_{\text{eff-I}}^+(\omega) = \left[1 - 2\frac{\omega_M}{\omega} + \left(1 + 2\frac{\omega_M}{\omega} \right) e^{-\frac{\omega}{\omega_M}} \right] \frac{\phi_B^+(\omega)}{\omega^2}, \\ \phi_{\text{eff-II}}^+(\omega) = \left[1 - 2\frac{\omega_M}{\omega} + 2\frac{\omega_M}{\omega} e^{-\frac{\omega}{\omega_M}} \right] \frac{\phi_B^+(\omega)}{\omega^2}, \\ \phi_{\text{eff-III}}^+(\omega) = \left[\left(1 + \frac{\omega_M}{\omega} \right) e^{-\frac{\omega}{\omega_M}} - 1 \right] \frac{\phi_B^+(\omega)}{\omega^2}. \quad (3.43)$$

Collecting the different pieces of the NLP contributions that we estimated above, the total NLP correction to the $B \rightarrow K^*$ form factors in QCD is expressed as

$$F_{BK^*,\text{NLP}}^i = F_{BK^*,\text{NLP}}^{i,\text{HT}} + F_{BK^*,\text{NLP}}^{i,\text{QPE}} + F_{BK^*,\text{NLP}}^{i,\text{HQE}} + F_{BK^*,\text{NLP}}^{i,\text{4P}}, \quad (3.44)$$

where the index “ i ” refers to seven different $B \rightarrow K^*$ form factors in QCD. Before proceeding to the numerical analysis, we first investigate the power counting rule of the form factors at LP and NLP, adopting the asymptotic behaviors of B -meson LCDAs [46]. According to the power-counting scheme $\omega_M \sim \omega_s \sim \mathcal{O}(\lambda^2)$ and $m_s \sim \mathcal{O}(\lambda)$ that employed in Ref. [13] with the units $\lambda = \Lambda_{\text{QCD}}/m_b$, we can derive the scaling rule for leading-power $B \rightarrow K^*$ form factors,

$$\begin{aligned} V_{BK^*}^{\text{LP}} &\sim A_{1,BK^*}^{\text{LP}} \sim T_{1,BK^*}^{\text{LP}} \sim T_{2,BK^*}^{\text{LP}} \sim \mathcal{O}(\lambda^2), \\ A_{0,BK^*}^{\text{LP}} &\sim \mathcal{O}(\lambda^3), \quad A_{12,BK^*}^{\text{LP}} \sim T_{23,BK^*}^{\text{LP}} \sim \mathcal{O}(\lambda^4), \end{aligned} \quad (3.45)$$

where A_{12} and T_{23} denote the combinations of the form factors corresponding to $\frac{m_B+m_V}{n \cdot p} A_1 - \frac{m_B-m_V}{m_B} A_2$ and $\frac{m_B}{n \cdot p} T_2 - T_3$, respectively. With the relations between seven QCD form factors and four SCET effective form factors in Ref. [24], the scaling of the form factors V, A_1, T_1, T_2 are decided by the SCET effective form factor ξ_\perp , while A_0, A_{12}, T_{23} are decided by the SCET effective form factor ξ_\parallel . Apparently, ξ_\parallel is suppressed with the power of λ^2 compared to ξ_\perp . Because A_0 has an enhanced factor $1/m_s$, it ultimately contributes the power of $\mathcal{O}(\lambda^3)$. Adopting the same analytical method as the leading power and the asymptotic behavior of two-particle and three-particle higher-twist B -meson LCDAs, we can also get the scaling of $B \rightarrow K^*$ form factors at NLP

$$\begin{aligned} V_{BK^*}^{\text{NLP}} &\sim A_{1,BK^*}^{\text{NLP}} \sim T_{1,BK^*}^{\text{NLP}} \sim T_{2,BK^*}^{\text{NLP}} \sim \mathcal{O}(\lambda^3), \\ A_{0,BK^*}^{\text{NLP}} &\sim \mathcal{O}(\lambda^4), \quad A_{12,BK^*}^{\text{NLP}} \sim T_{23,BK^*}^{\text{NLP}} \sim \mathcal{O}(\lambda^5). \end{aligned} \quad (3.46)$$

4 Numerical analysis

Summing up both the NLL correction and the newly derived NLP corrections, we obtain the SCET sum rule improved $B \rightarrow K^*$ form factors in the large recoil region. In this section, we analyze phenomenological observables for the cleanest FCNC process $B \rightarrow K^* \nu_\ell \bar{\nu}_\ell$. We first list the relevant theoretical inputs in the factorization formula for the heavy-to-light form factors, including quark masses, decay constants, distribution amplitudes, sum rule parameters, electroweak parameters, and the inverse moment λ_B of the leading-twist B -meson LCDA from a recent lattice QCD simulations [52]. After taking into account both the available lattice QCD results in the high q^2 region and improved LCSR predictions in the low q^2 region, we then perform a combined fit to get the coefficients in the BCL z -series parametrization [32–36], and extend the $B \rightarrow K^*$ form factors to the entire kinematic region. Taking advantage of the newly updated LCSR predictions, we investigate the differential branching ratio and longitudinal K^* polarization fraction of $B \rightarrow K^* \nu_\ell \bar{\nu}_\ell$ decays. For $B^+ \rightarrow K^{*+} \nu_\ell \bar{\nu}_\ell$ decay process, the additional long-distance effect induced by $B^+ \rightarrow \tau^+ (\rightarrow K^{*+} \nu_\tau) \bar{\nu}_\tau$ at tree level is included in the narrow τ width approximation [53]. It is emphasised that the uncertainties of our final theoretical predictions of $B \rightarrow K^* \nu_\ell \bar{\nu}_\ell$ are reduced to the level of 10% by adopting the λ_B from the lattice QCD simulation and carrying out the BCL fits.

4.1 Theory inputs

In Tab. 1, we summarize the necessary input parameters of the Standard Model and relevant hadronic parameters, along with the central values and uncertainties. In our numerical calculations, we employ the three-loop evolution of the strong coupling constant $\alpha_s(\mu)$ in the $\overline{\text{MS}}$ scheme by taking the interval $\alpha_s^{(5)}(m_Z)$ from [54] and adopting the perturbative matching scales $\mu_4 = 4.8\text{GeV}$ and

$\mu_4 = 1.3\text{GeV}$ for crossing the $n_f = 4$ and $n_f = 3$ thresholds, respectively [47, 55]. Additionally, the bottom quark mass $m_b(m_b)$ and strange quark mass $m_s(m_s)$ are given in the $\overline{\text{MS}}$ scheme at the scale of their respective $\overline{\text{MS}}$ masses. Taking advantage of **RunDec** [56], we obtain the scale dependence of the strong coupling constant $\alpha_s(\mu)$, as well as the quark masses $m_b(\mu)$ and $m_s(\mu)$. Moreover, we incorporate the results from four-flavor lattice QCD computations for the B -meson decay constant f_B [57]. The longitudinal decay constant of the K^* can be extracted from leptonic decays $V^0 \rightarrow e^+e^-$ and tau lepton decays $\tau^+ \rightarrow V^+\nu_\tau$, while the renormalization scale-dependent transverse decay constant of the K^* is taken from a lattice QCD simulation with $2 + 1$ flavors of domain wall quarks and the Iwasaki gauge action [58]. Two hard scales μ_{h1} and μ_{h2} are introduced in the hard functions and B -meson decay constants, respectively. The factorization scale μ is the same as the hard-collinear scale and the renormalization scale for the QCD tensor current will be taken as $\nu = m_b$.

For the LCSR improved form factors of the B -meson semileptonic decay process, B -meson LCDAs are the universal non-perturbative input parameters. Therefore, we need to construct an acceptable phenomenological model for the leading- and higher-twist B -meson LCDAs that not only satisfies the classical equations of motion [46], but also show the expected asymptotic behavior at sufficiently large scales. In this work, we adopt a newly proposed three-parameter model for all the relevant B -meson light-cone distribution amplitudes in coordinate space [59], with the details provided in Appendix D. The three shape parameters α , β and ω_0 in this model can be related to the (logarithmic) inverse moments λ_B and $\hat{\sigma}_{1,2}$ for the leading-twist B -meson distribution amplitude ϕ_B^+ with the equations

$$\begin{aligned}\lambda_B(\mu) &= \frac{\alpha - 1}{\beta - 1} \omega_0, \\ \hat{\sigma}_1(\mu) &= \psi(\beta - 1) - \psi(\alpha - 1) + \ln \frac{\alpha - 1}{\beta - 1}, \\ \hat{\sigma}_2(\mu) &= \hat{\sigma}_1^2(\mu) + \psi'(\alpha - 1) - \psi'(\beta - 1) + \frac{\pi^2}{6},\end{aligned}\tag{4.1}$$

and the definitions of the (logarithmic) inverse moments λ_B and $\hat{\sigma}_{1,2}$ are

$$\begin{aligned}\frac{1}{\lambda_B(\mu)} &= \int_0^\infty \frac{d\omega}{\omega} \phi_B^+(\omega, \mu), \\ \frac{\hat{\sigma}_n(\mu)}{\lambda_B(\mu)} &= \int_0^\infty \frac{d\omega}{\omega} \ln^n \frac{e^{-\gamma_E} \lambda_B(\mu)}{\omega} \phi_B^+(\omega, \mu).\end{aligned}\tag{4.2}$$

The numerical values for the hadronic parameters λ_B , $\hat{\sigma}_{1,2}$ and $\lambda_{E,H}$ in Tab. 1 are all given at the reference scale $\mu_0 = 1\text{ GeV}$ and these parameters will be evolved to the factorization scale μ in the final results. Although various strategies are employed to investigate the inverse moment λ_B [59–62], so far, we have not been able to establish a QCD-based method to provide a precise determination of λ_B since it is defined by a nonlocal operator (see Refs. [52, 63] for preliminary results from the lattice QCD perspectives). As suggested by the recent lattice QCD result [52, 63], we adopt $\lambda_B(1\text{GeV}) = (389 \pm 35)\text{ MeV}$ in this work, which will reduce the uncertainties of the form factors by 20% compared to the conservative interval of $\lambda_B = (350 \pm 150)\text{ MeV}$ [48, 55]. For the logarithmic inverse moments $\hat{\sigma}_{1,2}$, we prefer the choice $\{\hat{\sigma}_1, \hat{\sigma}_2\} = \{0, \pi^2/6\}$ with the intervals

$$-0.7 < \hat{\sigma}_1 < 0.7, \quad -6.0 < \hat{\sigma}_2 < 6.0,\tag{4.3}$$

suggested from the study of the $\gamma^* \rightarrow \pi\gamma$ transition [29, 30, 59].

Following the standard procedure outlined in Refs. [22, 24, 64], the two intrinsic parameters ω_M and ω_s introduced by the light-cone sum rules can be determined by effectively constraining

the smallness of the continuum contributions in the dispersion integrals and the stability of the obtained sum rule results against the variation of ω_M . The parameters s_0^\perp and s_0^\parallel correspond to the interpolating currents $\bar{q}'\not{p}\gamma_\perp q$ and $\bar{q}'\not{p}q$, which leads to the following intervals

$$\begin{aligned} s_0^\perp &= n \cdot p \omega_s^\perp = (1.4 \pm 0.1) \text{ GeV}^2, & s_0^\parallel &= n \cdot p \omega_s^\parallel = (1.7 \pm 0.1) \text{ GeV}^2, \\ M^2 &= n \cdot p \omega_M = (1.7 \pm 0.5) \text{ GeV}^2. \end{aligned} \quad (4.4)$$

Table 1. Numerical values of the input parameters that determines the $B \rightarrow K^*$ form factors.

Parameter	Value	Ref.	Parameter	Value	Ref.
m_{B^0}	5279.66 MeV	[54]	$m_{K^{*0}}$	898.46 MeV	[54]
m_{B^+}	5279.34 MeV	[54]	$m_{K^{*+}}$	891.67 MeV	[54]
τ_{B^0}	1.517(4) ps	[54]	τ_{B^+}	1.638(4) ps	[54]
m_{τ^+}	1776.86 MeV	[54]	τ_{τ^+}	0.2903(5) ps	[54]
G_F	$1.166379 \times 10^{-5} \text{ GeV}^{-2}$	[54]	$\sin^2 \theta_W$	0.23126(5)	[65]
$ V_{tb}V_{ts}^* $	$(41.25 \pm 0.45) \times 10^{-3}$	[66]	$\alpha_{em}(m_Z)$	1/127.925	[54]
$ V_{ub} $	$3.82(20) \times 10^{-3}$	[54]	$ V_{us} $	0.2243(8)	[54]
$m_b(m_b)$	$(4.203 \pm 0.011) \text{ GeV}$	[54]	$m_s(m_s)$	$(93.5 \pm 0.8) \text{ MeV}$	[54]
f_B	$(190.0 \pm 1.3) \text{ MeV}$	[57]	μ_{h1}	$[m_b/2, 2m_b]$	
$f_{K^*}^\parallel$	$(204 \pm 7) \text{ MeV}$	[5]	μ_{h2}	$[m_b/2, 2m_b]$	
$f_{K^*}^\perp(1\text{Gev})$	$(159 \pm 6) \text{ MeV}$	[58]	μ	$1.5 \pm 0.5 \text{ GeV}$	
$\langle \bar{q}q \rangle(2\text{Gev})$	$-(286 \pm 23 \text{ MeV})^3$	[57]	ν	m_b	
$\langle \bar{s}s \rangle : \langle \bar{q}q \rangle$	(0.8 ± 0.1)	[67, 68]	M^2	$(1.7 \pm 0.5) \text{ GeV}^2$	[64]
s_0^\parallel	$(1.7 \pm 0.1) \text{ GeV}^2$	[22, 64]	s_0^\perp	$(1.4 \pm 0.1) \text{ GeV}^2$	[22, 64]
λ_B	$389 \pm 35 \text{ MeV}$	[52, 63]		$\{0.7, 6.0\}$	
$(\lambda_E^2/\lambda_H^2)$	0.50 ± 0.10	[59]	$\{\hat{\sigma}_1, \hat{\sigma}_2\}$	$\{0.0, \pi^2/6\}$	[55]
$(2\lambda_E^2 + \lambda_H^2)$	$(0.25 \pm 0.15) \text{ GeV}^2$	[59]		$\{-0.7, -6.0\}$	

Table 2. The $B \rightarrow K^*$ form factors at $q^2 = 0$ given by our work (second row) and by sum rules with light-meson distribution amplitudes (third row).

$\mathcal{F}_i^{B \rightarrow K^*}$	\mathcal{V}	\mathcal{A}_0	\mathcal{A}_1	\mathcal{T}_1	\mathcal{T}_2	\mathcal{A}_{12}	\mathcal{T}_{23}
This work	0.15(11)	0.051(29)	0.14(10)	0.17(12)	0.14(11)	0.051(29)	0.076(34)
Ref. [5]	0.29(3)	0.118(16)	0.306(33)	0.282(31)	0.274(31)	0.113(15)	0.095(13)

4.2 Numerical predictions for the $B \rightarrow K^*$ form factors

Making use of the numerical inputs from Tab. 1 and the B -meson light-cone distribution amplitudes described by three-parameter model in the Appendix D, we obtain the $B \rightarrow K^*$ form factors in the large recoil region. In Tab. 2, we present the numerical values of $B \rightarrow K^*$ form factors based on LCSR with heavy-meson distribution amplitudes at $q^2 = 0$. The central values of our improved form factors are consistent within $1\sim 2\sigma$ deviation with the results derived by sum rules based on K^* distribution amplitudes [5]. To observe the numerical features of the LCSR parameters to form factors, we firstly present the dependence of the form factors on the Borel mass M^2 in Fig. 4. The left panel in Fig. 4 shows the variation of form factor \mathcal{V} when the Borel mass M^2 changes within the range of 1.2 GeV^2 to 2.2 GeV^2 , with the effective threshold s_0^\perp fixed at 1.3 GeV^2 , 1.4 GeV^2 , and 1.5 GeV^2 , respectively. The right panel in Fig. 4 illustrates the effect on the form factor \mathcal{A}_0 for the same Borel mass range, with the effective threshold set at 1.6 GeV^2 , 1.7 GeV^2 , and 1.8 GeV^2 , respectively. We find that LCSR form factors exhibit a mild dependence on the intrinsic parameters M^2 and $s_0^{\parallel,\perp}$ and the two LCSR parameters will introduce 10% systematic uncertainties to the form factors, respectively, which is consistent with our previous work [24] and other sum rule results [29, 30].

We are now ready to explore the contributions of the subleading-power corrections from different sources to the $B \rightarrow K^*$ form factors and focus on the form factors \mathcal{V} and \mathcal{A}_0 as examples. In Fig. 5, we explicitly display the contributions of four different sources of the subleading-power corrections as well as the total power correction in the kinematic region of $0 \leq q^2 \leq 6 \text{ GeV}^2$. These subleading-power corrections include the ‘‘HT’’ contribution from the two-particle and three-particle higher-twist B -meson distribution amplitudes, the ‘‘QPE’’ contribution from the expansion of hard-collinear quark propagator in the small parameter Λ_{QCD}/m_b , the ‘‘HQE’’ contribution from the power-suppressed effective weak transition current $\bar{q}\Gamma[i\hat{D}_\perp/(2m_b)]h_v$, and the ‘‘4P’’ contribution from twist-5 and twist-6 four-particle B -meson LCDAs within the factorization approach. We can observe that the NLP contribution from twist-5 and twist-6 four-particle B -meson LCDAs is minimal for the $B \rightarrow K^*$ form factors and this contribution accounts for only 3% \sim 7% of the total NLP contribution for the form factors \mathcal{V} and \mathcal{A}_0 , respectively. In contrast, it is evident that the higher-twist B -meson LCDAs provide the largest contributions to the NLP $B \rightarrow K^*$ form factors, which numerically account for 50% \sim 60% of the total NLP corrections in analogy to the previous discussions [29, 30, 69].

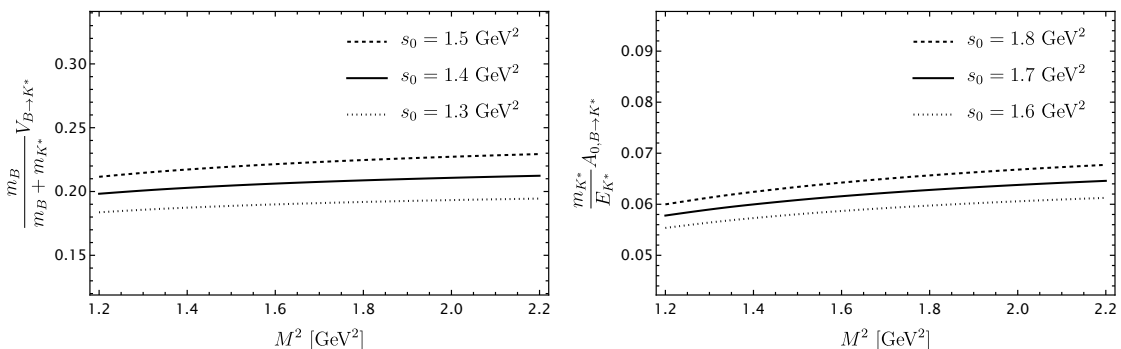


Figure 4. Form factors $\mathcal{V}_{B \rightarrow K^*}$ and $\mathcal{A}_{0, B \rightarrow K^*}$ dependence on the Borel parameters M^2 .

Now we proceed to explore the contribution of the NLL resummation improved leading-power $B \rightarrow K^*$ form factors and the newly derived subleading-power correction to the $B \rightarrow K^*$ form factors at tree level. In order to understand the impact of one-loop and subleading-power corrections, we illustrate the explicit numerical results for the resummation improved contribution at

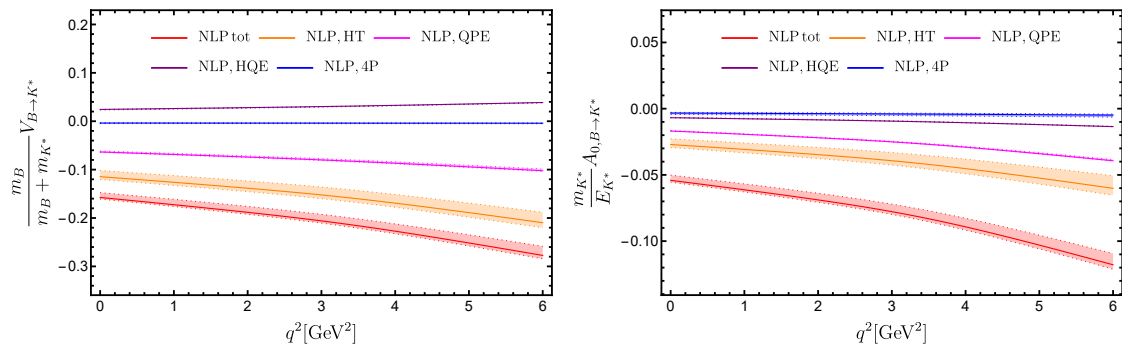


Figure 5. Different sources of subleading-power corrections to the $B \rightarrow K^*$ form factors $\mathcal{V}_{B \rightarrow K^*}$ (left panel) and $\mathcal{A}_{0, B \rightarrow K^*}$ (right panel) in the kinematic region of $0 \leq q^2 \leq 6 \text{ GeV}^2$. The error bands indicate the uncertainties for the variation of factorization scale μ .

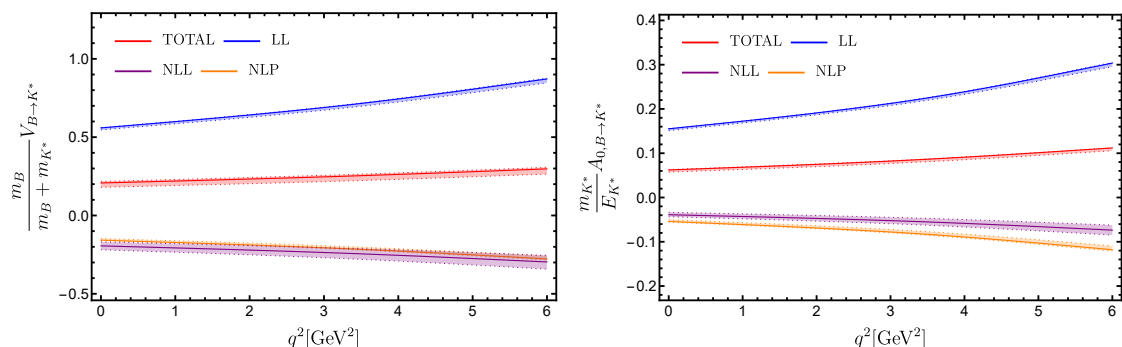


Figure 6. The comparison of LL resummation improved tree level contribution (LL), NLL resummation improved one-loop correction (NLL), subleading-power correction at tree level (NLP) and total result (TOTAL) to the $B \rightarrow K^*$ form factors $\mathcal{V}_{B \rightarrow K^*}$ (left panel) and $\mathcal{A}_{0, B \rightarrow K^*}$ (right panel) in the kinematic region of $0 \leq q^2 \leq 6 \text{ GeV}^2$. The error bands indicate the uncertainties for the variation of factorization scale μ .

one-loop level and NLP corrections at the tree level to the $B \rightarrow K^*$ form factors in the region of $0 \leq q^2 \leq 6 \text{ GeV}^2$ in Fig. 6. Taking the form factors \mathcal{V} and \mathcal{A}_0 as examples, the resummation improved NLL correction reduces the form factors \mathcal{V} and \mathcal{A}_0 by 30% compared to the results at leading-logarithm accuracy. Besides, the newly determined NLP corrections will cause a roughly 30% decrease to the form factors \mathcal{V} and \mathcal{A}_0 , respectively. After accounting for both NLP and NLL corrections, we find that the total results for the form factors \mathcal{V} and \mathcal{A}_0 will show a 60% reduction of the corresponding LL resummation improved tree-level predictions.

In addition, we investigate the dependence of both the NLL resummation improved one-loop correction and NLP correction derived in this work on the inverse moment λ_B at $q^2 = 0$. We set $\{\hat{\sigma}_1, \hat{\sigma}_2\} = \{0, \pi^2/6\}$ as central value and the corresponding numerical results are displayed in Fig. 7. Taking the form factors \mathcal{V} and \mathcal{A}_0 as examples, it is clear that both the NLL resummation improved one-loop correction and NLP correction stabilize the λ_B dependence of the $B \rightarrow K^*$ form factors. In contrast, the LL resummation improved tree-level results and the predictions of the total $B \rightarrow K^*$ form factors show an evident dependence on λ_B , which highlights the importance of an accurate determination of λ_B . It is worth noting that the areas with deeper color correspond to the latest recommended lattice QCD prediction of $\lambda_B = 0.389(35) \text{ GeV}$ [52, 63]. By adopting $\lambda_B = 0.389(35) \text{ GeV}$ rather than conservative interval $\lambda_B = 0.350(150) \text{ GeV}$ [59], the uncertainty of the form factors can be reduced by 20%, and the dominant source of theoretical uncertainty

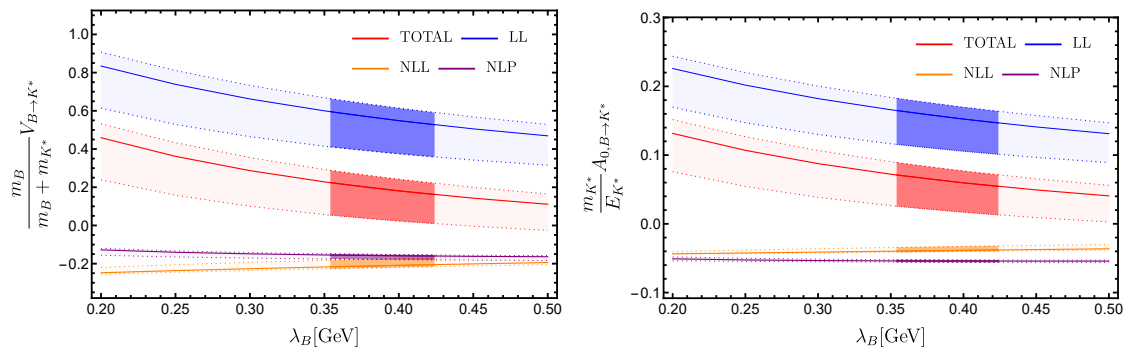


Figure 7. The comparison of LL resummation improved tree level contribution (LL), NLL resummation improved one-loop correction (NLL), subleading-power correction at tree level (NLP) and total result (TOTAL) to the $B \rightarrow K^*$ form factors $\mathcal{V}_{B \rightarrow K^*}$ (left panel) and $\mathcal{A}_{0,B \rightarrow K^*}$ (right panel) with the variation of $0.2 \text{ GeV} \leq \lambda_B \leq 0.5 \text{ GeV}$. The areas with deeper color correspond to $\lambda_B = 0.389(35) \text{ GeV}$. The upper (lower) bound represents $\{\hat{\sigma}_1, \hat{\sigma}_2\} = \{-0.7, -6.0\}$ ($\{\hat{\sigma}_1, \hat{\sigma}_2\} = \{0.7, 6.0\}$).

arises from the variation of the first two modified logarithmic inverse moments of the leading twist distribution amplitude $\{\hat{\sigma}_1, \hat{\sigma}_2\}$, which range from $\{0.7, 6\}$ to $\{-0.7, -6\}$.

Since our LCSR predictions are valid only in the large recoil region $0 \leq q^2 \leq 6 \text{ GeV}^2$, we have to extrapolate the LCSR calculations of the $B \rightarrow K^*$ form factors to the entire kinematic region of q^2 by employing the BCL z -series expansion based upon the positivity and analyticity properties of these transition form factors [32–36]. Applying the conformal transformation

$$z(q^2, t_0) = \frac{\sqrt{t_+ - q^2} - \sqrt{t_+ - t_0}}{\sqrt{t_+ - q^2} + \sqrt{t_+ - t_0}} \quad (4.5)$$

with the threshold parameter $t_+ \equiv (m_B + m_{K^*})^2$ for the exclusive $B \rightarrow K^*$ form factors, allows us to map the complex cut q^2 -plane onto the unit disk $|z(q^2, t_0)| \leq 1$. Besides, the free parameter $t_0 < t_+$ refers to the value of q^2 mapping onto the origin in the z -plane. In order to reduce the interval of z , the free parameter t_0 is taken as

$$t_0 = t_+ - \sqrt{t_+(t_+ - t_-)}, \quad t_- = (m_B - m_{K^*})^2. \quad (4.6)$$

Considering the asymptotic behavior of the form factor near the threshold of the corresponding excited states, we can further parameterize the $B \rightarrow K^*$ form factors with the z -series expansion as follows

$$\mathcal{F}_{B \rightarrow K^*}^i(q^2) = \frac{1}{1 - q^2/m_{i,pole}^2} \sum_{k=0}^{N-1} b_k^i [z(q^2, t_0) - z(0, t_0)]^k, \quad (4.7)$$

where $m_{i,pole}^2$ denotes the masses of the corresponding resonances below the particle-pair production threshold $(m_B + m_{K^*})$ with different quantum numbers. For convenience, we have summarized the masses of the resonances relevant to our parameterization in Tab. 3 following Ref. [5]. We will truncate the z -series expansion at $N = 3$ in the subsequent fitting process, the contribution after the quadratic terms is negligible due to $|z|_{\max} < 0.1$.

We are now in the position to determine the z -series coefficients $b_{0,1,2}^i$ of the $B \rightarrow K^*$ form factors $\mathcal{F}^i(q^2)$ by performing the correlated minimal- χ^2 fit of the updated LCSR predictions in the large recoil region in combination with the available lattice QCD data in the small recoil region [9, 10]. The ingredients of the minimal- χ^2 fit can be summarized as:

Table 3. Summary of the resonance masses with different quantum numbers entering the z -series expansions of the $B \rightarrow K^*$ form factors in Eq. (4.7).

$\mathcal{F}_{B \rightarrow K^*}^i(q^2)$	J^P	$m_{i,pole}$ [GeV]
$\mathcal{V}(q^2), \mathcal{T}_1(q^2)$	1^-	5.415
$\mathcal{A}_0(q^2)$	0^-	5.366
$\mathcal{A}_1(q^2), \mathcal{A}_{12}(q^2), \mathcal{T}_2(q^2), \mathcal{T}_{23}(q^2)$	1^+	5.829

- In the low q^2 region, we generate the improved LCSR form factors with uncertainties at three distinct kinematic points $q^2 = \{-4, 0, 4\} \text{ GeV}^2$. In order to obtain the pseudo-data samples, we vary the theoretical input parameters randomly within the error ranges and generate an ensemble of $N = 300$ parameter sets that obey uncorrelated priors, which are either uniform or Gaussian distributed [31].
- We multiply each form factor $\mathcal{F}_{\text{LCSR}}^i(q^2)$ by an enhancement factor $W_K = 1.09(1)$ to account for the finite K^* width effect in $B \rightarrow K^*$ transition, as discussed in Refs. [27, 70]. In the lattice QCD simulation, K^* is a stable particle [9, 10].
- In the high q^2 region, we reproduce the central values and correlation matrix of the lattice QCD results of the $B \rightarrow K^*$ form factors at three different points $q^2 = \{12, 14, 16\} \text{ GeV}^2$ with the data provided in lattice QCD computations [9, 10] as well as physical-mass bottom quark and $2 + 1$ flavors of sea quarks. To ensure the positive definiteness of the correlation matrix from the lattice QCD results, we modify the original matrix by adding an additional $\mathcal{O}(10^{-6})$ diagonal matrix, namely $C_{\text{latt}} = C_{\text{latt,original}} + 10^{-6}$.
- Taking into account the kinematic constraints,

$$\frac{m_B + m_V}{2m_V} A_1(0) - \frac{m_B - m_V}{2m_V} A_2(0) = A_0(0), \quad T_1(0) = T_2(0), \quad (4.8)$$

we can derive the following exact relations between the expansion coefficients,

$$\frac{m_V^2}{m_B^2 + m_V^2} b_0^{A_1} - \frac{2m_B^2 + m_V^2}{m_B^2 + m_V^2} b_0^{A_{12}} = b_0^{A_0}, \quad \frac{m_B^2}{m_B^2 + m_V^2} b_0^{T_1} = b_0^{T_2}. \quad (4.9)$$

- We then construct

$$\begin{aligned} \chi^2 = & \sum_{ij} [\mathcal{F}_{\text{LCSR}}^i(q^2) - \mathcal{F}_{\text{fit}}^i(q^2; b_k^i)] (C_{\text{LCSR}}^{ij})^{-1} [\mathcal{F}_{\text{LCSR}}^j(q^2) - \mathcal{F}_{\text{fit}}^j(q^2; b_k^j)] \\ & + \sum_{ij} [\mathcal{F}_{\text{latt}}^i(q^2) - \mathcal{F}_{\text{fit}}^i(q^2; b_k^i)] (C_{\text{latt}}^{ij})^{-1} [\mathcal{F}_{\text{latt}}^j(q^2) - \mathcal{F}_{\text{fit}}^j(q^2; b_k^j)], \end{aligned} \quad (4.10)$$

where \mathcal{F}^i denote the central values of the form factors and C^{ij} is the corresponding covariance matrix. We then extract the central values and the covariance of the coefficients b_k^i by minimizing the χ^2 function with $\chi_{\text{min}}^2/\text{d.o.f} = 56.1/23$. Our inputs as well as the fit results of z -series coefficients, including the central values, uncertainties and all correlations, will be presented on the arXiv page as supplemental material.

In order to further clarify the momentum-transfer dependence of the updated LCSR predictions and lattice QCD results, we display the combined fit for the seven $B \rightarrow K^*$ form factors in the

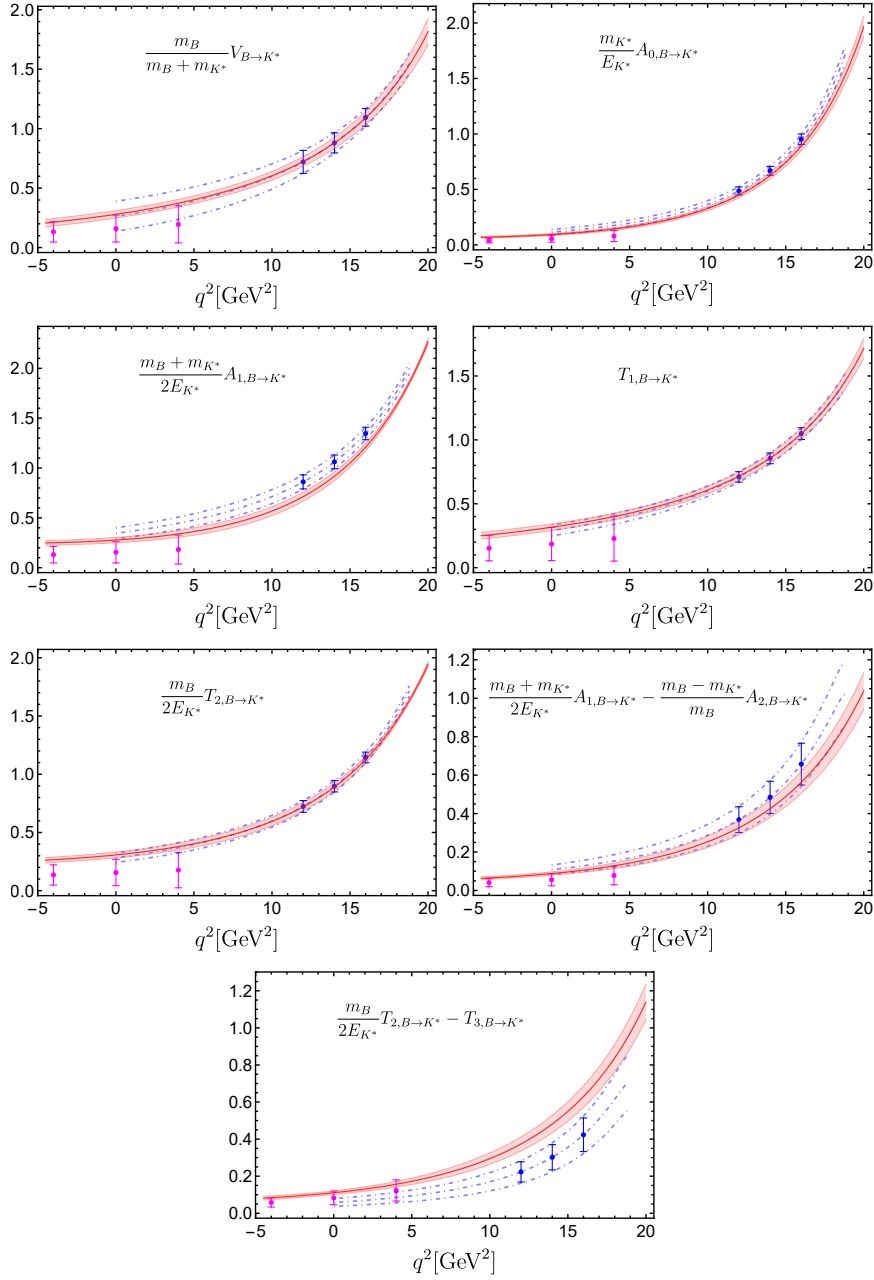


Figure 8. Theoretical predictions of the $B \rightarrow K^*$ decay form factors (red band) obtained from combined fit of updated LCSR (pink points) and lattice QCD (blue points) in the entire kinematical region. The “lattice QCD only” predictions for these form factors are indicated by the blue dot-dashed line for a comparison [9, 10].

entire kinematic region in Fig. 8, where the red band represents the combined fit results of BCL parameterization applied to our updated LCSR data (pink points) and lattice QCD data (blue points). For comparison, we also show the counterpart predictions of the $B \rightarrow K^*$ form factors from the lattice QCD data points with blue dot-dashed line [9, 10]. It is evident that including the newly derived LCSR data points in the low q^2 region in the process of combined fit to both LCSR

results and lattice QCD simulation significantly improves the accuracy of theoretical predictions for the $B \rightarrow K^*$ form factors across the entire momentum region.

4.3 Phenomenological analysis of the $B \rightarrow K^* \nu_\ell \bar{\nu}_\ell$ observables

The $B \rightarrow K^* \nu_\ell \bar{\nu}_\ell$ decays induced by the $b \rightarrow s$ flavor-changing neutral current (FCNC) are one of the cleanest decay channels. We now start to explore the phenomenological implications of the newly determined $B \rightarrow K^*$ form factors on the electroweak penguin $B \rightarrow K^* \nu_\ell \bar{\nu}_\ell$ decays. Thanks to the high luminosity of the Belle II experiment, the exclusive rare $B \rightarrow K^* \nu_\ell \bar{\nu}_\ell$ decays are expected to be observed with 10 ab^{-1} of the data [71, 72] and the earlier experimental measurements by BaBar [73] and Belle [74, 75] are also presented here. Importantly, the expected resolutions of the total branching fraction for the $B \rightarrow K^* \nu_\ell \bar{\nu}_\ell$ with 50 ab^{-1} of integrated luminosity is estimated to reach a level of around 10%, thus making the experimental results comparable to the current theoretical uncertainty of the Standard Model prediction. Furthermore, the longitudinal K^* polarization fraction, which is highly sensitive to right-handed currents [71], can also be measured with an error of 0.1.

We are therefore well motivated to investigate the phenomenological aspects of the $B \rightarrow K^* \nu_\ell \bar{\nu}_\ell$ process further, both to gain a better understanding of the strong interaction dynamics of the $B \rightarrow K^*$ form factors and to explore the potential role of exotic particles X in the dark matter context, using the here derived form factors. It is straightforward to derive the differential decay width formula [6, 76]

$$\begin{aligned} \frac{d\Gamma(B \rightarrow K^* \nu_\ell \bar{\nu}_\ell)}{dq^2} &= \frac{G_F^2 \alpha_{em}^2 \lambda^{3/2}(m_B^2, m_{K^*}^2, q^2)}{256 \pi^5 m_B^3 \sin^4 \theta_W} |\lambda_t|^2 \left[X_t \left(\frac{m_t^2}{m_W^2}, \frac{m_H^2}{m_t^2}, \sin \theta_W, \mu \right) \right]^2 \\ &\times \left[H_V(q^2) + H_{A_1}(q^2) + H_{A_{12}}(q^2) \right], \end{aligned} \quad (4.11)$$

where $\lambda(x, y, z) = x^2 + y^2 + z^2 - 2xy - 2xz - 2yz$ is the Källén function. The CKM matrix elements $\lambda_t = |V_{tb} V_{ts}^*|$ can be determined by the **UT fit** collaboration [66] and the input parameters appearing in the differential decay width are collected in Tab. 1. The short-distance Wilson coefficient X_t can be expanded perturbatively in terms of the Standard Model coupling constants

$$X_t = X_t^{(0)} + \frac{\alpha_s}{4\pi} X_t^{\text{QCD}(1)} + \frac{\alpha_{em}}{4\pi} X_t^{\text{EW}(1)} + \dots, \quad (4.12)$$

where the LO contribution $X_t^{(0)}$ [77], the NLO QCD correction $X_t^{\text{QCD}(1)}$ [78–80] and the two-loop electroweak correction $X_t^{\text{EW}(1)}$ [65] are already known analytically. We take the value of $X_t = 1.469$ in our work. The three invariant functions H_i can be further expressed by the $B \rightarrow K^*$ form factors as

$$\begin{aligned} H_V(q^2) &= \frac{2q^2}{(m_B + m_{K^*})^2} [V(q^2)]^2, \\ H_{A_1}(q^2) &= \frac{2q^2(m_B + m_{K^*})^2}{\lambda(m_B^2, m_{K^*}^2, q^2)} [A_1(q^2)]^2, \\ H_{A_{12}}(q^2) &= \frac{64m_B^2 m_{K^*}^2}{\lambda(m_B^2, m_{K^*}^2, q^2)} [A_{12}(q^2)]^2, \end{aligned} \quad (4.13)$$

with the helicity form factors A_{12} [9]

$$A_{12}(q^2) = \frac{(m_B + m_{K^*})^2 (m_B^2 - m_{K^*}^2 - q^2) A_1(q^2) - \lambda(m_B^2, m_{K^*}^2, q^2) A_2(q^2)}{16m_B m_{K^*}^2 (m_B + m_{K^*})}. \quad (4.14)$$

To probe new physics effects beyond the SM, λ_t is usually evaluated using CKM unitarity.

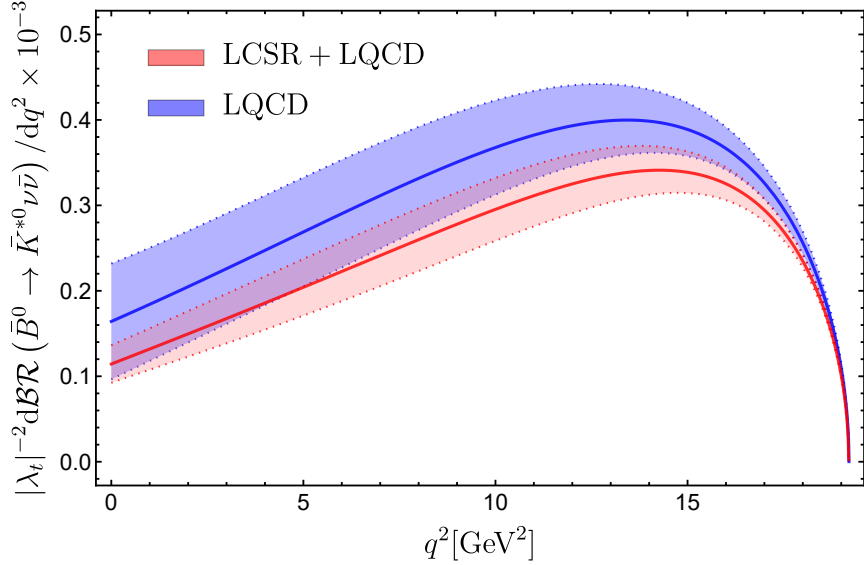


Figure 9. Theory predictions for the CKM-independent differential branching fraction of $B^0 \rightarrow K^{*0} \nu_\ell \bar{\nu}_\ell$ by applying the form factors determined from the combined fits (pink band) and from the lattice simulations (blue band) [9, 10].

However, the CKM coupling V_{cb} extracted by different processes is not consistent (see Ref. [7] for further discussions). For future reference, we present the CKM-independent branching ratio $|\lambda_t|^{-2} \mathcal{BR}(B^0 \rightarrow K^{*0} \nu_\ell \bar{\nu}_\ell)$ estimated with various strategies in Tab. 4. The branching ratios derived from updated $B \rightarrow K^*$ form factors are consistent within a 2.5σ deviation with the results derived by sum rules based on K^* distribution amplitudes [5]. We also display in Fig. 9 yielding our theoretical prediction for the CKM-independent differential branching fraction of $B^0 \rightarrow K^{*0} \nu_\ell \bar{\nu}_\ell$ and show the result from lattice QCD calculations for comparison. It is evident that the combined fit result has significantly smaller uncertainty compared to those from lattice QCD data in the entire momentum region. We give our final numerical results for differential branching ratio of $B \rightarrow K^* \nu_\ell \bar{\nu}_\ell$ in Tab. 5 by using $\lambda_t = 41.25 \times 10^{-3}$ as noted above. All the uncertainty is dominated by uncertainties of hadronic form factors.

Table 4. The CKM-independent branching ratio of $B^0 \rightarrow K^{*0} \nu_\ell \bar{\nu}_\ell$ process from updated form factors (left), lattice QCD FFs (mid) and LCSRs with K^* -meson LCDAs (right).

$10^{-3} \times (\lambda_t)^{-2} \mathcal{BR}$	This work	Ref. [9, 10]	Ref. [5]
$B^0 \rightarrow K^{*0} \nu_\ell \bar{\nu}_\ell$	4.43(50)	5.86(93)	5.85(58)

There is an additional long-distance (LD) contribution to the counterpart channel $B^+ \rightarrow K^{*+} \nu_\ell \bar{\nu}_\ell$ with a charged B -meson due to the double-charged current interaction $B^+ \rightarrow \tau^+ (\rightarrow K^{*+} \nu_\tau) \bar{\nu}_\tau$ as originally discussed in Ref. [53]. In the narrow τ -lepton width limit, we write the tree-level LD contribution to the differential decay rate

$$\begin{aligned} \frac{d\Gamma(B^+ \rightarrow K^{*+} \nu_\ell \bar{\nu}_\ell)}{dq^2} \Big|_{\text{LD}} &= \frac{G_F^4 |V_{ub} V_{us}^*|^2}{64\pi^2 m_B^3} |f_B f_{K^*}|^2 \frac{m_\tau^3}{\Gamma_\tau} \\ &\times [(m_B^2 - m_\tau^2)(m_\tau^2 - m_{K^*}^2) - (m_\tau^2 - 2m_{K^*}^2)q^2], \end{aligned} \quad (4.15)$$

This long-distance effect arising from weak annihilation mediated by the on-shell τ -lepton accounts

for 10% of the electroweak penguin contribution, which is numerically significant for the charged channel $B^+ \rightarrow K^{*+} \nu_\ell \bar{\nu}_\ell$ [71]. Moreover, the interference effect between the tree and penguin amplitudes turns out to be negligible numerically on account for extremely small τ -lepton width [53].

We then proceed to define the differential longitudinal K^* polarization fraction F_L of the electroweak penguin $B \rightarrow K^* \nu_\ell \bar{\nu}_\ell$ decays

$$F_L(q^2) = \frac{H_{A_{12}}(q^2)}{H_V(q^2) + H_{A_1}(q^2) + H_{A_{12}}(q^2)}. \quad (4.16)$$

In addition, we also introduce two q^2 -binned observables for the comparison with the future high-luminosity Belle II data

$$\begin{aligned} \Delta\mathcal{BR}(q_1^2, q_2^2) &= \tau_B \int_{q_1^2}^{q_2^2} dq^2 \frac{d\Gamma(B \rightarrow K^* \nu_\ell \bar{\nu}_\ell)}{dq^2}, \\ \Delta F_L(q_1^2, q_2^2) &= \frac{\int_{q_1^2}^{q_2^2} dq^2 \lambda^{3/2}(m_B^2, m_{K^*}^2, q^2) H_{A_{12}}(q^2)}{\int_{q_1^2}^{q_2^2} dq^2 \lambda^{3/2}(m_B^2, m_{K^*}^2, q^2) [H_V(q^2) + H_{A_1}(q^2) + H_{A_{12}}(q^2)]}. \end{aligned} \quad (4.17)$$

Our predictions for these quantities with the choice of q^2 -intervals following [71] are summarized in Tab. 5. The theoretical uncertainties of the q^2 -binned longitudinal K^* polarization fractions ΔF_L are much reduced compared to the resulting predictions of $\Delta\mathcal{BR}$, due to the reduced sensitivity of the form-factor ratios to the precise shapes of the B -meson distribution amplitudes.

Table 5. Theory predictions for the integrated differential observables $\Delta\mathcal{BR}(q_1^2, q_2^2)$, and $\Delta F_L(q_1^2, q_2^2)$ obtained from the exclusive $B \rightarrow K^*$ form factors and additional long-distance contribution.

$[q_1^2, q_2^2]$ (in GeV^2)	$10^6 \times \Delta\mathcal{BR}^{B^0 \rightarrow K^{*0} \nu_\ell \bar{\nu}_\ell}(q_1^2, q_2^2)$	$10^6 \times \Delta\mathcal{BR}^{B^+ \rightarrow K^{*+} \nu_\ell \bar{\nu}_\ell}(q_1^2, q_2^2)$	$\Delta F_L(q_1^2, q_2^2)$
[0.0, 1.0]	0.194(37)	0.290(41)	0.93(2)
[1.0, 2.5]	0.343(62)	0.487(69)	0.80(4)
[2.5, 4.0]	0.407(71)	0.551(78)	0.68(5)
[4.0, 6.0]	0.64(11)	0.84(12)	0.59(5)
[6.0, 8.0]	0.76(12)	0.95(13)	0.50(5)
[8.0, 12.0]	1.86(24)	2.25(26)	0.41(4)
[12.0, 16.0]	2.12(19)	2.50(20)	0.34(2)
$[16.0, (m_B - m_{K^*})^2]$	1.217(57)	1.487(65)	0.31(1)
$[0.0, (m_B - m_{K^*})^2]$	7.54(86)	9.35(94)	0.44(4)

5 Conclusions

In this work, we have comprehensively investigated the subleading-power corrections to the $B \rightarrow K^*$ form factors within the framework of light-cone sum rules (LCSR) with B -meson LCDAs. The corrections are generated by two-particle and three-particle B -meson higher-twist light-cone distribution amplitudes, by the power-suppressed terms in the expansion of the strange quark propagator, by the subleading-power effective current $\bar{q}\Gamma[i\mathcal{D}_\perp/(2m_b)]h_v$ in HQET, and by the four-particle twist-five and twist-six B -meson LCDAs in the factorization approximation. By combining

the leading power contribution at NLL accuracy from Ref. [24] and our newly derived NLP contributions, we ultimately obtain updated predictions for the $B \rightarrow K^*$ form factors with SCET sum rules in the large recoil region. It is clearly shown that the power correction accounts for approximately 30% correction to the tree level result, which is comparable to the NLL contribution. Moreover, we find that the dominant source of power corrections arises from the two-particle higher-twist B -meson LCDAs, while the impact of the four-particle corrections is numerically insignificant.

Then we adopted the three-parameter model to describe the leading-twist and higher-twist B -meson LCDAs, incorporating the latest lattice QCD prediction for the inverse moment $\lambda_B = 0.389(35)$ GeV [52, 63]. Compared to the conservative interval $\lambda_B = 0.350(150)$ GeV [48, 55], the new result from the lattice QCD reduces the uncertainties of the $B \rightarrow K^*$ form factors by approximately 20%. By adopting the BCL parameterization and performing a combined fit of the newly derived LCSR predictions in the low q^2 region and the lattice QCD results in the high q^2 region [9, 10], we extrapolate the $B \rightarrow K^*$ form factors to the entire momentum region. We found that the $B \rightarrow K^*$ form factors derived from the combined fits exhibit smaller uncertainties compared to those with only lattice data points. Furthermore, the combined fits to the LCSR and lattice QCD input of the $B \rightarrow K^*$ form factors not only provide predictions for the form factors that are applicable across the entire kinematic range, but also verify the consistency of the two complementary methods by ensuring their coincidence at intermediate q^2 values. Notably, the results show good agreement between the two approaches. Having at our disposal the $B \rightarrow K^*$ form factors in the entire momentum region, we proceed to predict the differential decay widths for $B \rightarrow K^* \nu_\ell \bar{\nu}_\ell$ processes, including the long-distance effects in the charged $B \rightarrow K^* \nu_\ell \bar{\nu}_\ell$ decay process. Furthermore, we display the CKM-independent differential branching ratio of $B^0 \rightarrow K^{*0} \nu_\ell \bar{\nu}_\ell$ obtained from the combined fits alongside the lattice simulation result for comparison. The results with different fit data inputs are consistent with each other and the combined fits to the differential branching ratio of $B^0 \rightarrow K^{*0} \nu_\ell \bar{\nu}_\ell$ provide smaller uncertainties. Finally, we obtain the branching ratios $\mathcal{BR}(\bar{B}^0 \rightarrow \bar{K}^{*0} \nu_\ell \bar{\nu}_\ell) = 7.54(86) \times 10^{-6}$, $\mathcal{BR}(\bar{B}^+ \rightarrow \bar{K}^{*+} \nu_\ell \bar{\nu}_\ell) = 9.35(94) \times 10^{-6}$ and the longitudinal K^* polarization fraction $F_L = 0.44(4)$.

For the $b \rightarrow s$ induced flavor-changing neutral current processes, a crucial task is to improve the precision of the $B \rightarrow K^*$ form factors. It can be further improved with respect to the following three aspects: it would be essential for us to accurately describe the B -meson light-cone distribution amplitudes with model-independent methods. Reducing the uncertainties of the non-perturbative input parameters, such as the inverse moment λ_B of the leading-twist B -meson LCDA, is indispensable for improving the precision of form factors. Then the perturbative calculations can be extended to higher precision, such as advancing the current computations to next-to-next-to-leading order at the leading power or to the next-to-leading order at the subleading power. Finally, it can provide additional theoretical constraints by imposing stricter unitarity bounds in the process of z -series parameterization, which can further reduce the uncertainties of the form factors.

Ultimately, we want to emphasize that our improved $B \rightarrow K^*$ form factors are crucial for investigating flavor-changing neutral current processes and determining the branching ratios of the electroweak penguin process $B \rightarrow K^* \nu_\ell \bar{\nu}_\ell$. With the high luminosity Belle II experimental data provided, our predictions will be further tested in the future.

Acknowledgements

We thank Shan Cheng for valuable discussions. Yue-Long Shen acknowledges support from the National Natural Science Foundation of China with Grant No. 12175218, and the Natural Science Foundation of Shandong Province under the Grant No. ZR2024MA076. Dong-Hao Li acknowledges support from the National Natural Science Foundation of China with Grant No. 12447154. The

work of UGM was supported in part by the CAS President's International Fellowship Initiative (PIFI) under Grant No. 2025PD0022.

References

- [1] M. Algueró, A. Biswas, B. Capdevila, S. Descotes-Genon, J. Matias and M. Novoa-Brunet, *To (b)e or not to (b)e: no electrons at LHCb*, *Eur. Phys. J. C* **83** (2023) 648, [[2304.07330](#)].
- [2] LHCb collaboration, R. Aaij et al., *Measurement of CP-Averaged Observables in the $B^0 \rightarrow K^{*0} \mu^+ \mu^-$ Decay*, *Phys. Rev. Lett.* **125** (2020) 011802, [[2003.04831](#)].
- [3] B. Capdevila, A. Crivellin and J. Matias, *Review of semileptonic B anomalies*, *Eur. Phys. J. ST* **1** (2023) 20, [[2309.01311](#)].
- [4] BELLE-II collaboration, I. Adachi et al., *Evidence for $B^+ \rightarrow K^+ \nu \nu^-$ decays*, *Phys. Rev. D* **109** (2024) 112006, [[2311.14647](#)].
- [5] A. Bharucha, D. M. Straub and R. Zwicky, *$B \rightarrow V \ell^+ \ell^-$ in the Standard Model from light-cone sum rules*, *JHEP* **08** (2016) 098, [[1503.05534](#)].
- [6] A. J. Buras, J. Girrbach-Noe, C. Niehoff and D. M. Straub, *$B \rightarrow K^{(*)} \nu \bar{\nu}$ decays in the Standard Model and beyond*, *JHEP* **02** (2015) 184, [[1409.4557](#)].
- [7] D. Bečirević, G. Piazza and O. Sumensari, *Revisiting $B \rightarrow K^{(*)} \nu \bar{\nu}$ decays in the Standard Model and beyond*, *Eur. Phys. J. C* **83** (2023) 252, [[2301.06990](#)].
- [8] B.-F. Hou, X.-Q. Li, M. Shen, Y.-D. Yang and X.-B. Yuan, *Deciphering the Belle II data on $B \rightarrow K \nu \bar{\nu}$ decay in the (dark) SMEFT with minimal flavour violation*, *JHEP* **06** (2024) 172, [[2402.19208](#)].
- [9] R. R. Horgan, Z. Liu, S. Meinel and M. Wingate, *Lattice QCD calculation of form factors describing the rare decays $B \rightarrow K^* \ell^+ \ell^-$ and $B_s \rightarrow \phi \ell^+ \ell^-$* , *Phys. Rev. D* **89** (2014) 094501, [[1310.3722](#)].
- [10] R. R. Horgan, Z. Liu, S. Meinel and M. Wingate, *Rare B decays using lattice QCD form factors*, *PoS LATTICE2014* (2015) 372, [[1501.00367](#)].
- [11] M. Beneke and T. Feldmann, *Symmetry breaking corrections to heavy to light B meson form-factors at large recoil*, *Nucl. Phys. B* **592** (2001) 3–34, [[hep-ph/0008255](#)].
- [12] C. W. Bauer, D. Pirjol and I. W. Stewart, *Factorization and endpoint singularities in heavy to light decays*, *Phys. Rev. D* **67** (2003) 071502, [[hep-ph/0211069](#)].
- [13] M. Beneke and T. Feldmann, *Factorization of heavy to light form-factors in soft collinear effective theory*, *Nucl. Phys. B* **685** (2004) 249–296, [[hep-ph/0311335](#)].
- [14] M. Beneke, A. P. Chapovsky, M. Diehl and T. Feldmann, *Soft collinear effective theory and heavy to light currents beyond leading power*, *Nucl. Phys. B* **643** (2002) 431–476, [[hep-ph/0206152](#)].
- [15] R. J. Hill, T. Becher, S. J. Lee and M. Neubert, *Sudakov resummation for subleading SCET currents and heavy-to-light form-factors*, *JHEP* **07** (2004) 081, [[hep-ph/0404217](#)].
- [16] M. Beneke and D. Yang, *Heavy-to-light B meson form-factors at large recoil energy: Spectator-scattering corrections*, *Nucl. Phys. B* **736** (2006) 34–81, [[hep-ph/0508250](#)].
- [17] C. W. Bauer, S. Fleming, D. Pirjol and I. W. Stewart, *An Effective field theory for collinear and soft gluons: Heavy to light decays*, *Phys. Rev. D* **63** (2001) 114020, [[hep-ph/0011336](#)].
- [18] M. Beneke, Y. Kiyo and D. s. Yang, *Loop corrections to subleading heavy quark currents in SCET*, *Nucl. Phys. B* **692** (2004) 232–248, [[hep-ph/0402241](#)].
- [19] P. Ball and V. M. Braun, *Use and misuse of QCD sum rules in heavy to light transitions: The Decay $B \rightarrow \rho e \nu$ reexamined*, *Phys. Rev. D* **55** (1997) 5561–5576, [[hep-ph/9701238](#)].

- [20] P. Ball and V. M. Braun, *Exclusive semileptonic and rare B meson decays in QCD*, *Phys. Rev. D* **58** (1998) 094016, [[hep-ph/9805422](#)].
- [21] P. Ball and R. Zwicky, *$B_{d,s} \rightarrow \rho, \omega, K^*, \phi$ decay form-factors from light-cone sum rules revisited*, *Phys. Rev. D* **71** (2005) 014029, [[hep-ph/0412079](#)].
- [22] A. Khodjamirian, T. Mannel and N. Offen, *Form-factors from light-cone sum rules with B-meson distribution amplitudes*, *Phys. Rev. D* **75** (2007) 054013, [[hep-ph/0611193](#)].
- [23] A. Khodjamirian, T. Mannel, A. A. Pivovarov and Y. M. Wang, *Charm-loop effect in $B \rightarrow K^{(*)} \ell^+ \ell^-$ and $B \rightarrow K^* \gamma$* , *JHEP* **09** (2010) 089, [[1006.4945](#)].
- [24] J. Gao, C.-D. Lü, Y.-L. Shen, Y.-M. Wang and Y.-B. Wei, *Precision calculations of $B \rightarrow V$ form factors from soft-collinear effective theory sum rules on the light-cone*, *Phys. Rev. D* **101** (2020) 074035, [[1907.11092](#)].
- [25] A. Khodjamirian, B. Melić and Y.-M. Wang, *A guide to the QCD light-cone sum rules for b-quark decays*, *Eur. Phys. J. ST* **233** (2024) 271–298, [[2311.08700](#)].
- [26] S. Cheng, A. Khodjamirian and J. Virto, *Timelike-helicity $B \rightarrow \pi\pi$ form factor from light-cone sum rules with dipion distribution amplitudes*, *Phys. Rev. D* **96** (2017) 051901, [[1709.00173](#)].
- [27] S. Descotes-Genon, A. Khodjamirian and J. Virto, *Light-cone sum rules for $B \rightarrow K\pi$ form factors and applications to rare decays*, *JHEP* **12** (2019) 083, [[1908.02267](#)].
- [28] S. Descotes-Genon, A. Khodjamirian, J. Virto and K. K. Vos, *Light-Cone Sum Rules for S-wave $B \rightarrow K\pi$ Form Factors*, *JHEP* **06** (2023) 034, [[2304.02973](#)].
- [29] B.-Y. Cui, Y.-K. Huang, Y.-L. Shen, C. Wang and Y.-M. Wang, *Precision calculations of $B_{d,s} \rightarrow \pi, K$ decay form factors in soft-collinear effective theory*, *JHEP* **03** (2023) 140, [[2212.11624](#)].
- [30] J. Gao, T. Huber, Y. Ji, C. Wang, Y.-M. Wang and Y.-B. Wei, *$B \rightarrow D\ell\nu_\ell$ form factors beyond leading power and extraction of $-V_{cb}$ and $R(D)$* , *JHEP* **05** (2022) 024, [[2112.12674](#)].
- [31] B.-Y. Cui, Y.-K. Huang, Y.-M. Wang and X.-C. Zhao, *Shedding new light on $R(D(s)^{(*)})$ and $-V_{cb}$ from semileptonic $B^-(s) \rightarrow D(s)^{(*)} \ell \nu^- \ell$ decays*, *Phys. Rev. D* **108** (2023) L071504, [[2301.12391](#)].
- [32] S. Okubo, *New improved bounds for k-l-3 parameters*, *Phys. Rev. D* **4** (1971) 725–733.
- [33] C. Bourrely, B. Machet and E. de Rafael, *Semileptonic Decays of Pseudoscalar Particles ($M \rightarrow M' \ell \nu_\ell$) and Short Distance Behavior of Quantum Chromodynamics*, *Nucl. Phys. B* **189** (1981) 157–181.
- [34] L. Lellouch, *Lattice constrained unitarity bounds for anti- $B_0 \rightarrow \pi^+ \ell \nu^-$ decays*, *Nucl. Phys. B* **479** (1996) 353–391, [[hep-ph/9509358](#)].
- [35] C. Bourrely and I. Caprini, *Bounds on the slope and the curvature of the scalar $K \pi$ form-factor at zero momentum transfer*, *Nucl. Phys. B* **722** (2005) 149–165, [[hep-ph/0504016](#)].
- [36] C. Bourrely, I. Caprini and L. Lellouch, *Model-independent description of $B \rightarrow \pi l \nu$ decays and a determination of $-V(ub)$* , *Phys. Rev. D* **79** (2009) 013008, [[0807.2722](#)].
- [37] F. De Fazio, T. Feldmann and T. Hurth, *Light-cone sum rules in soft-collinear effective theory*, *Nucl. Phys. B* **733** (2006) 1–30, [[hep-ph/0504088](#)].
- [38] F. De Fazio, T. Feldmann and T. Hurth, *SCET sum rules for $B \rightarrow P$ and $B \rightarrow V$ transition form factors*, *JHEP* **02** (2008) 031, [[0711.3999](#)].
- [39] Y.-M. Wang and Y.-L. Shen, *QCD corrections to $B \rightarrow \pi$ form factors from light-cone sum rules*, *Nucl. Phys. B* **898** (2015) 563–604, [[1506.00667](#)].
- [40] C.-D. Lü, Y.-L. Shen, Y.-M. Wang and Y.-B. Wei, *QCD calculations of $B \rightarrow \pi, K$ form factors with higher-twist corrections*, *JHEP* **01** (2019) 024, [[1810.00819](#)].

- [41] M. Beneke and T. Feldmann, *Multipole expanded soft collinear effective theory with nonAbelian gauge symmetry*, *Phys. Lett. B* **553** (2003) 267–276, [[hep-ph/0211358](#)].
- [42] A. G. Grozin and M. Neubert, *Asymptotics of heavy meson form-factors*, *Phys. Rev. D* **55** (1997) 272–290, [[hep-ph/9607366](#)].
- [43] P. Colangelo and A. Khodjamirian, *QCD sum rules, a modern perspective*, [hep-ph/0010175](#).
- [44] M. Beneke and J. Rohrwild, *B meson distribution amplitude from $B \rightarrow \gamma l \nu$* , *Eur. Phys. J. C* **71** (2011) 1818, [[1110.3228](#)].
- [45] I. I. Balitsky and V. M. Braun, *Evolution Equations for QCD String Operators*, *Nucl. Phys. B* **311** (1989) 541–584.
- [46] V. M. Braun, Y. Ji and A. N. Manashov, *Higher-twist B-meson Distribution Amplitudes in HQET*, *JHEP* **05** (2017) 022, [[1703.02446](#)].
- [47] Y.-L. Shen, Y.-M. Wang and Y.-B. Wei, *Precision calculations of the double radiative bottom-meson decays in soft-collinear effective theory*, *JHEP* **12** (2020) 169, [[2009.02723](#)].
- [48] C. Wang, Y.-M. Wang and Y.-B. Wei, *QCD factorization for the four-body leptonic B-meson decays*, *JHEP* **02** (2022) 141, [[2111.11811](#)].
- [49] M. Neubert, *Heavy quark symmetry*, *Phys. Rept.* **245** (1994) 259–396, [[hep-ph/9306320](#)].
- [50] A. F. Falk, M. Neubert and M. E. Luke, *The Residual mass term in the heavy quark effective theory*, *Nucl. Phys. B* **388** (1992) 363–375, [[hep-ph/9204229](#)].
- [51] S. S. Agaev, V. M. Braun, N. Offen and F. A. Porkert, *Light Cone Sum Rules for the π^0 - γ Form Factor Revisited*, *Phys. Rev. D* **83** (2011) 054020, [[1012.4671](#)].
- [52] X.-Y. Han et al., *Calculation of heavy meson light-cone distribution amplitudes from lattice QCD*, [2410.18654](#).
- [53] J. F. Kamenik and C. Smith, *Tree-level contributions to the rare decays $B^+ \rightarrow \pi^+ \nu \text{ anti-}\nu$, $B^+ \rightarrow K^+ \nu \text{ anti-}\nu$, and $B^+ \rightarrow K^{*+} \nu \text{ anti-}\nu$ in the Standard Model*, *Phys. Lett. B* **680** (2009) 471–475, [[0908.1174](#)].
- [54] PARTICLE DATA GROUP collaboration, S. Navas et al., *Review of particle physics*, *Phys. Rev. D* **110** (2024) 030001.
- [55] M. Beneke, C. Bobeth and Y.-M. Wang, *$B_{d,s} \rightarrow \gamma \ell \bar{\ell}$ decay with an energetic photon*, *JHEP* **12** (2020) 148, [[2008.12494](#)].
- [56] K. G. Chetyrkin, J. H. Kuhn and M. Steinhauser, *RunDec: A Mathematica package for running and decoupling of the strong coupling and quark masses*, *Comput. Phys. Commun.* **133** (2000) 43–65, [[hep-ph/0004189](#)].
- [57] FLAVOUR LATTICE AVERAGING GROUP (FLAG) collaboration, Y. Aoki et al., *FLAG Review 2021*, *Eur. Phys. J. C* **82** (2022) 869, [[2111.09849](#)].
- [58] RBC-UKQCD collaboration, C. Allton et al., *Physical Results from 2+1 Flavor Domain Wall QCD and $SU(2)$ Chiral Perturbation Theory*, *Phys. Rev. D* **78** (2008) 114509, [[0804.0473](#)].
- [59] M. Beneke, V. M. Braun, Y. Ji and Y.-B. Wei, *Radiative leptonic decay $B \rightarrow \gamma l \nu_\ell$ with subleading power corrections*, *JHEP* **07** (2018) 154, [[1804.04962](#)].
- [60] T. Janowski, B. Pullin and R. Zwicky, *Charged and neutral $\overline{B}_{u,d,s} \rightarrow \gamma$ form factors from light cone sum rules at NLO*, *JHEP* **12** (2021) 008, [[2106.13616](#)].
- [61] V. M. Braun, D. Y. Ivanov and G. P. Korchemsky, *The B meson distribution amplitude in QCD*, *Phys. Rev. D* **69** (2004) 034014, [[hep-ph/0309330](#)].
- [62] W. Wang, Y.-M. Wang, J. Xu and S. Zhao, *B-meson light-cone distribution amplitude from Euclidean quantities*, *Phys. Rev. D* **102** (2020) 011502, [[1908.09933](#)].

- [63] X.-Y. Han, J. Hua, X. Ji, C.-D. Lü, W. Wang, J. Xu et al., *A new method to access heavy meson lightcone distribution amplitudes from first-principle*, [2403.17492](#).
- [64] P. Ball, V. M. Braun, Y. Koike and K. Tanaka, *Higher twist distribution amplitudes of vector mesons in QCD: Formalism and twist - three distributions*, *Nucl. Phys. B* **529** (1998) 323–382, [[hep-ph/9802299](#)].
- [65] J. Brod, M. Gorbahn and E. Stamou, *Two-Loop Electroweak Corrections for the $K \rightarrow \pi\nu\bar{\nu}$ Decays*, *Phys. Rev. D* **83** (2011) 034030, [[1009.0947](#)].
- [66] UTFIT collaboration, M. Bona et al., *New UTfit Analysis of the Unitarity Triangle in the Cabibbo-Kobayashi-Maskawa scheme*, *Rend. Lincei Sci. Fis. Nat.* **34** (2023) 37–57, [[2212.03894](#)].
- [67] B. L. Ioffe, *Condensates in quantum chromodynamics*, *Phys. Atom. Nucl.* **66** (2003) 30–43, [[hep-ph/0207191](#)].
- [68] P. Gelhausen, A. Khodjamirian, A. A. Pivovarov and D. Rosenthal, *Decay constants of heavy-light vector mesons from QCD sum rules*, *Phys. Rev. D* **88** (2013) 014015, [[1305.5432](#)].
- [69] Y.-M. Wang and Y.-L. Shen, *Subleading-power corrections to the radiative leptonic $B \rightarrow \gamma\ell\nu$ decay in QCD*, *JHEP* **05** (2018) 184, [[1803.06667](#)].
- [70] S. Cheng, A. Khodjamirian and J. Virto, *$B \rightarrow \pi\pi$ Form Factors from Light-Cone Sum Rules with B -meson Distribution Amplitudes*, *JHEP* **05** (2017) 157, [[1701.01633](#)].
- [71] BELLE-II collaboration, W. Altmannshofer et al., *The Belle II Physics Book*, *PTEP* **2019** (2019) 123C01, [[1808.10567](#)].
- [72] BELLE-II collaboration, S. Halder, *Results and prospects of radiative and electroweak penguin decays at Belle II*, [2101.11573](#).
- [73] BABAR collaboration, J. P. Lees et al., *Search for $B \rightarrow K^{(*)}\nu\bar{\nu}$ and invisible quarkonium decays*, *Phys. Rev. D* **87** (2013) 112005, [[1303.7465](#)].
- [74] BELLE collaboration, O. Lutz et al., *Search for $B \rightarrow h^{(*)}\nu\bar{\nu}$ with the full Belle $\Upsilon(4S)$ data sample*, *Phys. Rev. D* **87** (2013) 111103, [[1303.3719](#)].
- [75] BELLE collaboration, J. Grygier et al., *Search for $B \rightarrow h\nu\bar{\nu}$ decays with semileptonic tagging at Belle*, *Phys. Rev. D* **96** (2017) 091101, [[1702.03224](#)].
- [76] W. Altmannshofer, A. J. Buras, D. M. Straub and M. Wick, *New strategies for New Physics search in $B \rightarrow K^{*}\nu\bar{\nu}$, $B \rightarrow K\nu\bar{\nu}$ and $B \rightarrow X_s\nu\bar{\nu}$ decays*, *JHEP* **04** (2009) 022, [[0902.0160](#)].
- [77] T. Inami and C. S. Lim, *Effects of Superheavy Quarks and Leptons in Low-Energy Weak Processes $k(L) \rightarrow \mu$ anti- μ , $K^+ \rightarrow \pi^+$ Neutrino anti-neutrino and $K^0 \leftrightarrow$ anti- K^0* , *Prog. Theor. Phys.* **65** (1981) 297.
- [78] G. Buchalla and A. J. Buras, *QCD corrections to the $\bar{s}dZ$ vertex for arbitrary top quark mass*, *Nucl. Phys. B* **398** (1993) 285–300.
- [79] G. Buchalla and A. J. Buras, *The rare decays $K \rightarrow \pi\nu\bar{\nu}$, $B \rightarrow X\nu\bar{\nu}$ and $B \rightarrow l^+l^-$: An Update*, *Nucl. Phys. B* **548** (1999) 309–327, [[hep-ph/9901288](#)].
- [80] M. Misiak and J. Urban, *QCD corrections to FCNC decays mediated by Z penguins and W boxes*, *Phys. Lett. B* **451** (1999) 161–169, [[hep-ph/9901278](#)].
- [81] T. Nishikawa and K. Tanaka, *QCD Sum Rules for Quark-Gluon Three-Body Components in the B Meson*, *Nucl. Phys. B* **879** (2014) 110–142, [[1109.6786](#)].
- [82] M. Rahimi and M. Wald, *QCD sum rules for parameters of the B -meson distribution amplitudes*, *Phys. Rev. D* **104** (2021) 016027, [[2012.12165](#)].
- [83] V. M. Braun, A. N. Manashov and N. Offen, *Evolution equation for the higher-twist B -meson distribution amplitude*, *Phys. Rev. D* **92** (2015) 074044, [[1507.03445](#)].

A Hard function for the SCET currents at $\mathcal{O}(\alpha_s)$

Here we present the hard coefficient functions of A0-type and B1-type SCET_I currents in $B \rightarrow K^*$ form factors up to $\mathcal{O}(\alpha_s)$

$$C_{f_+}^{(A0)} = 1 + \frac{\alpha_s C_F}{4\pi} \left\{ -2 \ln^2\left(\frac{r}{\hat{\mu}}\right) + 5 \ln\left(\frac{r}{\hat{\mu}}\right) - 2\text{Li}_2(1-r) - 3 \ln r - \frac{\pi^2}{12} - 6 \right\}, \quad (\text{A.1})$$

$$C_{f_0}^{(A0)} = 1 + \frac{\alpha_s C_F}{4\pi} \left\{ -2 \ln^2\left(\frac{r}{\hat{\mu}}\right) + 5 \ln\left(\frac{r}{\hat{\mu}}\right) - 2\text{Li}_2(1-r) - \frac{3-5r}{1-r} \ln r - \frac{\pi^2}{12} - 4 \right\}, \quad (\text{A.2})$$

$$C_{f_T}^{(A0)} = 1 + \frac{\alpha_s C_F}{4\pi} \left\{ -2 \ln \hat{\nu} - 2 \ln^2\left(\frac{r}{\hat{\mu}}\right) + 5 \ln\left(\frac{r}{\hat{\mu}}\right) - 2\text{Li}_2(1-r) - \frac{3-r}{1-r} \ln r - \frac{\pi^2}{12} - 6 \right\}, \quad (\text{A.3})$$

$$C_V^{(A0)} = 1 + \frac{\alpha_s C_F}{4\pi} \left\{ -2 \ln^2\left(\frac{r}{\hat{\mu}}\right) + 5 \ln\left(\frac{r}{\hat{\mu}}\right) - 2\text{Li}_2(1-r) - \frac{3-2r}{1-r} \ln r - \frac{\pi^2}{12} - 6 \right\}, \quad (\text{A.4})$$

$$C_{T_1}^{(A0)} = 1 + \frac{\alpha_s C_F}{4\pi} \left\{ -2 \ln \hat{\nu} - 2 \ln^2\left(\frac{r}{\hat{\mu}}\right) + 5 \ln\left(\frac{r}{\hat{\mu}}\right) - 2\text{Li}_2(1-r) - 3 \ln r - \frac{\pi^2}{12} - 6 \right\}, \quad (\text{A.5})$$

$$C_{f_+}^{(B1)} = (-2 + 1/r) + \mathcal{O}(\alpha_s), \quad C_{f_0}^{(B1)} = (-1/r) + \mathcal{O}(\alpha_s), \quad (\text{A.6})$$

$$C_{f_T}^{(B1)} = (1/r) + \mathcal{O}(\alpha_s), \quad C_V^{(B1)} = 0 + \mathcal{O}(\alpha_s), \quad C_{T_1}^{(B1)} = -1 + \mathcal{O}(\alpha_s), \quad (\text{A.7})$$

where we introduced three variables

$$r = \frac{n \cdot p}{m_b}, \quad \hat{\mu} = \frac{\mu}{m_b}, \quad \hat{\nu} = \frac{\nu}{m_b}. \quad (\text{A.8})$$

B Effective B -meson distribution amplitudes

$$\begin{aligned} \phi_{B,\text{eff}}^-(\omega', \mu) &= \phi_B^-(\omega', \mu) + \frac{\alpha_s C_F}{4\pi} \left\{ \int_0^{\omega'} d\omega \left[\frac{2}{\omega - \omega'} \left(\ln \frac{\mu^2}{n \cdot p\omega'} - 2 \ln \frac{\omega' - \omega}{\omega'} \right) \right]_{\oplus} \phi_B^-(\omega, \mu) \right. \\ &\left. - \int_{\omega'}^{\infty} d\omega \left[\ln^2 \frac{\mu^2}{n \cdot p\omega'} - \left(2 \ln \frac{\mu^2}{n \cdot p\omega'} + 3 \right) \ln \frac{\omega - \omega'}{\omega'} + 2 \ln \frac{\omega}{\omega'} + \frac{\pi^2}{6} - 1 \right] \frac{d\phi_B^-(\omega, \mu)}{d\omega} \right\}, \end{aligned} \quad (\text{B.1})$$

$$\begin{aligned} \tilde{\phi}_{B,\text{eff}}^-(\omega', \mu, \nu) &= \phi_B^-(\omega', \mu) + \frac{\alpha_s C_F}{4\pi} \left\{ \int_0^{\omega'} d\omega \left[\frac{2}{\omega - \omega'} \left(\ln \frac{\mu^2}{n \cdot p\omega'} - 2 \ln \frac{\omega' - \omega}{\omega'} - \frac{1}{2} \right) \right]_{\oplus} \phi_B^-(\omega, \mu) \right. \\ &\left. - \int_{\omega'}^{\infty} d\omega \left[\ln^2 \frac{\mu^2}{n \cdot p\omega'} - \ln \frac{\nu^2}{n \cdot p\omega'} - \left(2 \ln \frac{\mu^2}{n \cdot p\omega'} + 4 \right) \ln \frac{\omega - \omega'}{\omega'} + 2 \ln \frac{\omega}{\omega'} + \frac{\pi^2}{6} - 1 \right] \frac{d\phi_B^-(\omega, \mu)}{d\omega} \right\}, \end{aligned} \quad (\text{B.2})$$

$$\phi_{B,m}^+(\omega', \mu) = \frac{\alpha_s C_F}{4\pi} m_q \int_{\omega'}^{\infty} d\omega \ln \frac{\omega - \omega'}{\omega'} \frac{d\phi_B^+(\omega, \mu)}{d\omega}, \quad (\text{B.3})$$

the plus function appeared in the above equations is defined by

$$\int_0^{\omega'} d\omega [f(\omega, \omega')]_{\oplus} g(\omega) = \int_0^{\omega'} d\omega f(\omega, \omega') [g(\omega) - g(\omega')]. \quad (\text{B.4})$$

C Dispersion integral formula

After Borel transformation, the dispersion functions appearing in the factorization formula of $B \rightarrow K^*$ form factors are listed in the following

$$\begin{aligned}
f_{2,1}[\phi(\omega)] &= - \int_0^{\omega_s} d\omega e^{-\frac{\omega}{\omega_M}} \phi(\omega), \\
f_{2,2}[\phi(\omega)] &= e^{-\frac{\omega}{\omega_M}} \phi(\omega) + \int_0^{\omega_s} d\omega \frac{e^{-\frac{\omega}{\omega_M}}}{\omega_M} \phi(\omega), \\
f_{3,2}[\phi(\omega_1, \omega_2, u)] &= e^{-\frac{\omega_s}{\omega_M}} \int_0^{\omega_s} d\omega_1 \int_{\omega_s - \omega_1}^{\infty} \frac{d\omega_2}{\omega_2} \phi(\omega_1, \omega_2, \frac{\omega_s - \omega_1}{\omega_2}) \\
&\quad + \int_0^{\omega_s} d\omega \int_0^{\omega} d\omega_1 \int_{\omega - \omega_1}^{\infty} \frac{d\omega_2}{\omega_2} \frac{e^{-\frac{\omega_s}{\omega_M}}}{\omega_M} \phi(\omega_1, \omega_2, \frac{\omega - \omega_1}{\omega_2}), \tag{C.1} \\
f_{3,3}[\phi(\omega_1, \omega_2, u)] &= -\frac{1}{2} e^{\frac{\omega_s}{\omega_M}} \left\{ \int_{\omega_s}^{\infty} \frac{d\omega_2}{\omega_2} \phi\left(\frac{\omega_s}{\omega_2}, 0, \omega_2\right) \right. \\
&\quad \left. - \int_0^{\omega_s} d\omega_1 \int_{\omega_s - \omega_1}^{\infty} \frac{d\omega_2}{\omega_2} \left(\frac{d}{d\omega_1} - \frac{1}{\omega_M} \right) \phi\left(\omega_1, \omega_2, \frac{\omega_s - \omega_1}{\omega_2}\right) \right\} \\
&\quad - \frac{e^{-\frac{\omega_s}{\omega_M}}}{2\omega_M^2} \int_0^{\omega_s} d\omega \int_0^{\omega} d\omega_1 \int_{\omega - \omega_1}^{\infty} \frac{d\omega_2}{\omega_2} \phi\left(\omega_1, \omega_2, \frac{\omega - \omega_1}{\omega_2}\right),
\end{aligned}$$

where ϕ stands for the general B -meson LCDAs or its combinations entering the function $f_{i,j}$. And the function $f_{i,j}$ denotes the contribution of i -particle LCDA term with the power in the denominators $\phi(\omega)/(\omega - \dots)^j$.

D Modeling the B -meson LCDAs

The general ansatz for leading- and higher-twist B -meson LCDAs at the reference scale $\mu_0 = 1$ GeV can be systematically established [59] in such a way that both tree-level equations of motion constraints and the normalization conditions of the LCDAs [42, 46] are satisfied.

$$\begin{aligned}
\phi_B^+(\omega) &= \omega \mathbb{F}(\omega; -1), \quad \phi_B^{-\text{WW}}(\omega) = \mathbb{F}(\omega; 0), \\
\phi_B^{-\text{t3}}(\omega) &= \frac{1}{6} \mathcal{N} (\lambda_E^2 - \lambda_H^2) \left[-\omega^2 \mathbb{F}(\omega; -2) + 4\omega \mathbb{F}(\omega; -1) - 2\mathbb{F}(\omega; 0) \right], \\
\phi_3(\omega_1, \omega_2) &= \frac{1}{2} \mathcal{N} (\lambda_E^2 - \lambda_H^2) \omega_1 \omega_2^2 \mathbb{F}(\omega_1 + \omega_2; -2), \\
\widehat{g}_B^+(\omega) &= \frac{1}{4} \left[2\omega (\omega - \bar{\Lambda}) \mathbb{F}(\omega; 0) + (3\omega - 2\bar{\Lambda}) \mathbb{F}(\omega; 1) + 3\mathbb{F}(\omega; 2) \right. \\
&\quad \left. - \frac{1}{6} \mathcal{N} (\lambda_E^2 - \lambda_H^2) \omega^2 \mathbb{F}(\omega; 0) \right], \\
\widehat{g}_B^-(\omega) &= \frac{1}{4} \left\{ (3\omega - 2\bar{\Lambda}) \mathbb{F}(\omega; 1) + 3\mathbb{F}(\omega; 2) \right. \\
&\quad \left. + \frac{1}{3} \mathcal{N} (\lambda_E^2 - \lambda_H^2) \omega \left[\omega (\bar{\Lambda} - \omega) \mathbb{F}(\omega; -1) - \left(2\bar{\Lambda} - \frac{3}{2} \omega \right) \mathbb{F}(\omega; 0) \right] \right\}, \\
\phi_4(\omega_1, \omega_2) &= \frac{1}{2} \mathcal{N} (\lambda_E^2 + \lambda_H^2) \omega_2^2 \mathbb{F}(\omega_1 + \omega_2; -1), \\
\psi_4(\omega_1, \omega_2) &= \mathcal{N} \lambda_E^2 \omega_1 \omega_2 \mathbb{F}(\omega_1 + \omega_2; -1), \quad \widetilde{\psi}_4(\omega_1, \omega_2) = \mathcal{N} \lambda_H^2 \omega_1 \omega_2 \mathbb{F}(\omega_1 + \omega_2; -1), \\
\phi_5(\omega_1, \omega_2) &= \mathcal{N} (\lambda_E^2 + \lambda_H^2) \omega_1 \mathbb{F}(\omega_1 + \omega_2; 0), \quad \psi_5(\omega_1, \omega_2) = -\mathcal{N} \lambda_E^2 \omega_2 \mathbb{F}(\omega_1 + \omega_2; 0), \\
\widetilde{\psi}_5(\omega_1, \omega_2) &= -\mathcal{N} \lambda_H^2 \omega_2 \mathbb{F}(\omega_1 + \omega_2; 0),
\end{aligned}$$

$$\phi_6(\omega_1, \omega_2) = \mathcal{N}(\lambda_E^2 - \lambda_H^2) \mathbb{F}(\omega_1 + \omega_2; 1), \quad (\text{D.1})$$

where

$$\begin{aligned} \mathcal{N} &= \frac{1}{3} \frac{\beta(\beta+1)}{\alpha(\alpha+1)} \frac{1}{\omega_0^2}, & \bar{\Lambda} &= \frac{3}{2} \frac{\alpha}{\beta} \omega_0, \\ \mathbb{F}(\omega; n) &\equiv \omega_0^{n-1} U(\beta - \alpha, 2 - n - \alpha, \omega/\omega_0) \frac{\Gamma(\beta)}{\Gamma(\alpha)} e^{-\omega/\omega_0}, \end{aligned} \quad (\text{D.2})$$

with $U(a, b, z)$ is the hypergeometric U function. The appearing HQET parameters λ_E^2 and λ_H^2 at the reference scale $\mu_0 = 1$ GeV are defined by the matrix element of local quark-gluon-quark operator,

$$\begin{aligned} \langle 0 | \bar{q}(0) g_s G_{\mu\nu}(0) \Gamma h_v(0) | \bar{B}(v) \rangle &= -\frac{i}{6} \tilde{f}_B(\mu) m_B \lambda_H^2 \text{Tr} \left[\gamma_5 \Gamma P_+ \sigma_{\mu\nu} \right] \\ &\quad - \frac{1}{6} \tilde{f}_B(\mu) m_B \left(\lambda_H^2 - \lambda_E^2 \right) \text{Tr} \left[\gamma_5 \Gamma P_+ (v_\mu \gamma_\nu - v_\nu \gamma_\mu) \right]. \end{aligned} \quad (\text{D.3})$$

The matrix element can be estimated adopting QCD sum rules yielding,

$$\lambda_E^2 = 0.11 \pm 0.06 \text{ GeV}^2, \quad \lambda_H^2 = 0.18 \pm 0.07 \text{ GeV}^2, \quad [42] \quad (\text{D.4})$$

$$\lambda_E^2 = 0.03 \pm 0.02 \text{ GeV}^2, \quad \lambda_H^2 = 0.06 \pm 0.03 \text{ GeV}^2, \quad [81] \quad (\text{D.5})$$

$$\lambda_E^2 = 0.01 \pm 0.01 \text{ GeV}^2, \quad \lambda_H^2 = 0.15 \pm 0.05 \text{ GeV}^2, \quad [82] \quad (\text{D.6})$$

where we take into account that the method to estimate λ_E^2 and λ_H^2 as discussed in Ref. [82], unfortunately not only disrupt the convergence of the operator-product-expansion (OPE), but also enhance the contributions from the continuum and higher excited states. Therefore, we will use the numerical results of λ_E^2 and λ_H^2 from the Tab. 1, which can cover the ranges allowed by Ref. [42] and Ref. [81] and simultaneously satisfy the upper bounds imposed by Ref. [82].

We expect that the model for B -meson light-cone distribution amplitudes is only valid at the small momenta region and the (logarithmic) inverse moments are only sensitive to the small momentum behavior of the distribution amplitude. Employing the definitions of (logarithmic) inverse moments of the leading-twist B -meson LCDA

$$\begin{aligned} \frac{1}{\lambda_B(\mu)} &= \int_0^\infty \frac{d\omega}{\omega} \phi_B^+(\omega, \mu), \\ \frac{\hat{\sigma}_n(\mu)}{\lambda_B(\mu)} &= \int_0^\infty \frac{d\omega}{\omega} \ln^n \frac{e^{-\gamma_E} \lambda_B(\mu)}{\omega} \phi_B^+(\omega, \mu), \end{aligned} \quad (\text{D.7})$$

we can determine the parameters of three-parameter model for B -meson light-cone distribution amplitude (D.1)

$$\begin{aligned} \lambda_B(\mu) &= \frac{\alpha - 1}{\beta - 1} \omega_0, \\ \hat{\sigma}_1(\mu) &= \psi(\beta - 1) - \psi(\alpha - 1) + \ln \frac{\alpha - 1}{\beta - 1}, \\ \hat{\sigma}_2(\mu) &= \hat{\sigma}_1^2(\mu) + \psi'(\alpha - 1) - \psi'(\beta - 1) + \frac{\pi^2}{6}, \end{aligned} \quad (\text{D.8})$$

where γ_E and $\psi(x)$ denote the Euler-Mascheroni constant and the digamma function, respectively. The scale dependence of these moments at one-loop level read

$$\frac{\lambda_B(\mu_0)}{\lambda_B(\mu)} = 1 + \frac{\alpha_s(\mu_0) C_F}{4\pi} \ln \frac{\mu}{\mu_0} \left[2 - 2 \ln \frac{\mu}{\mu_0} - 4\sigma_1(\mu_0) \right],$$

$$\widehat{\sigma}_1(\mu) = \widehat{\sigma}_1(\mu_0) + \frac{\alpha_s(\mu_0) C_F}{4\pi} 4 \ln \frac{\mu}{\mu_0} \left[\widehat{\sigma}_1^2(\mu_0) - \widehat{\sigma}_2(\mu_0) \right]. \quad (\text{D.9})$$

Then we construct the LL resummation (evolution) for the twist-2 and 3 two-particle B -meson LCDAs. The explicit expressions can be found in Ref. [59]

$$\begin{aligned} \phi_B^+(\omega, \mu) &= U_\phi(\mu, \mu_0) \frac{1}{\omega^{p+1}} \frac{\Gamma(\beta)}{\Gamma(\alpha)} \mathcal{G}(\omega; 0, 2, 1), \\ \phi_B^{-\text{WW}}(\omega, \mu) &= U_\phi(\mu, \mu_0) \frac{1}{\omega^{p+1}} \frac{\Gamma(\beta)}{\Gamma(\alpha)} \mathcal{G}(\omega; 0, 1, 1), \\ \phi_B^{-\text{t}3}(\omega, \mu) &= -\frac{1}{6} U_\phi^{\text{t}3}(\mu, \mu_0) \mathcal{N} (\lambda_E^2 - \lambda_H^2) \frac{\omega_0^2}{\omega^{p+3}} \frac{\Gamma(\beta)}{\Gamma(\alpha)} \left\{ \mathcal{G}(\omega; 0, 3, 3) \right. \\ &\quad \left. + (\beta - \alpha) \left[\frac{\omega}{\omega_0} \mathcal{G}(\omega; 0, 2, 2) - \beta \frac{\omega}{\omega_0} \mathcal{G}(\omega; 1, 2, 2) - \mathcal{G}(\omega; 1, 3, 3) \right] \right\}, \end{aligned} \quad (\text{D.10})$$

where $p = \frac{\Gamma_{\text{cusp}}^{(0)}}{2\beta_0} \ln[\alpha_s(\mu)/\alpha_s(\mu_0)]$, the twist-3 two-particle LCDA $\phi_B^-(\omega, \mu) = \phi_B^{-\text{WW}}(\omega, \mu) + \phi_B^{-\text{t}3}(\omega, \mu)$ is a linear combination of the (twist-2) WW term and the genuine twist-3 term, and

$$\mathcal{G}(\omega; l, m, n) \equiv G_{23}^{21} \left(\frac{\omega}{\omega_0} \middle| \begin{matrix} 1, \beta + l \\ p + m, \alpha, p + n \end{matrix} \right), \quad (\text{D.11})$$

denotes the MeijerG function. The evolution factor $U_\phi(\mu, \mu_0)$ and $U_\phi^{\text{t}3}(\mu, \mu_0)$ reads explicitly at one-loop order [46, 83]

$$\begin{aligned} U_\phi(\mu, \mu_0) &= \exp \left\{ -\frac{\Gamma_{\text{cusp}}^{(0)}}{4\beta_0^2} \left(\frac{4\pi}{\alpha_s(\mu_0)} \left[\ln r - 1 + \frac{1}{r} \right] \right. \right. \\ &\quad \left. \left. - \frac{\beta_1}{2\beta_0} \ln^2 r + \left(\frac{\Gamma_{\text{cusp}}^{(1)}}{\Gamma_{\text{cusp}}^{(0)}} - \frac{\beta_1}{\beta_0} \right) [r - 1 - \ln r] \right) \right\} (e^{2\gamma_E} \mu_0)^{\frac{\Gamma_{\text{cusp}}^{(0)}}{2\beta_0} \ln r} r^{\frac{\gamma_{\text{t}2}^{(0)}}{2\beta_0}}, \\ U_\phi^{\text{t}3}(\mu, \mu_0) &= U_\phi(\mu, \mu_0) \Big|_{\gamma_{\text{t}2}^{(0)} \rightarrow \gamma_{\text{t}2}^{(0)} + \gamma_{\text{t}3}^{(0)}}, \end{aligned} \quad (\text{D.12})$$

where $r = \alpha_s(\mu)/\alpha_s(\mu_0)$, $\Gamma_{\text{cusp}}^{(i)}$ are the cusp anomalous dimensions at various orders and

$$\gamma_{\text{t}2}^{(0)} = -2C_F, \quad \gamma_{\text{t}3}^{(0)} = 2N_c. \quad (\text{D.13})$$

Both evolution factors satisfy the boundary condition at the reference scale μ_0

$$U_\phi(\mu_0, \mu_0) = 1, \quad U_\phi^{\text{t}3}(\mu_0, \mu_0) = 1. \quad (\text{D.14})$$